Epiretinal cell proliferation in macular pucker and vitreomacular traction syndrome:

Analysis of flat-mounted internal limiting membrane specimens

A thesis submitted for the degree of Doctor of Medicine
at the Faculty of Medicine
Ludwig-Maximilians-University Munich

Zhao, Fei

From
Tianjin, China

2012

Aus der Augenklinik und Poliklinik
der Ludwig-Maxmilians-Universität München
Direktor: Prof. Dr. med. Anselm Kampik

Epiretinale Zellproliferationen bei Macular pucker und vitreomakulärem Traktionssyndrom:

Untersuchung der inneren Grenzmembran als Flachpräparat

Dissertation
zum Erwerb des Doktorgrades der Medizin
an der Medizinischen Fakultät der
Ludwig-Maximilians-Universität zu München

vorgelegt von
Zhao, Fei

aus
Tianjin, China

2012

Mit Genehmigung der Medizinischen Fakultät
der Universität München

Berichterstatter:	Prof. Dr. med. Anselm Kampik
Mitberichterstatter:	Prof. Dr. med. Arnd Gandorfer
	Prof. Dr. med. Arthur Müller
Mitbetreuung durch den promovierten Mitarbeiter:	Dr. med. Ricarda G. Schumann
Dekan:	Prof. Dr. med. Dr. h.c. M. Reiser, FACR, FRCR
Tag der mündlichen Prüfung:	29. 03. 2012

天道酬勤

Ad Vitam Paramus

献给我亲爱的家人

For my beloved

Table of Contents

A. Abstracts

A.1 Summary

Macular pucker (MP) and vitreomacular traction syndrome (VMTS) are traction vitreoretinopathies that develop at the vitreoretinal interface of the macular area. The major component of the vitreoretinal interface is the internal limiting membrane (ILM), which is the site of epiretinal membrane (ERM) formation mediating tractional forces from the vitreous to retinal layers. Removal of the ILM/ERM represents a principal goal of vitreoretinal surgery in MP and VMTS. Recently, a new preparation method of surgically excised ILM specimens was proposed. The new flat-mount preparation method has numerous advantages compared to conventional cross-sectioning preparation procedures. Most importantly, it allows for showing the maximum area of a tissue specimen with en-face observation of the total cell distribution.

By using 119 flat-mounted ILM specimens with epiretinal tissue removed en-bloc during vitrectomy from eyes with MP and VMTS, we performed phase contrast and interference microscopy, LIVE/ DEAD viability assay, and indirect immunostaining by using 16 antibodies directed against glial cells, hyalocytes, retinal pigment epithelial cells, retinal ganglion cells and extracellular matrix components. The specimens were removed from 119 eyes of 117 patients including 79 eyes with MP and 40 eyes with VMTS. Intraoperatively, the state of the vitreous was assessed regarding the presence of complete or incomplete posterior vitreous detachment (PVD).

Since specimens from MP with complete PVD were found with significantly higher cell viability than specimens from MP with incomplete PVD and VMTS, we raise the hypothesis that the extent of PVD and the presence of vitreoretinal adhesions with traction forces at the retina may have some influence on cell viability of epiretinal cells. In this study, we found two cell distribution patterns. Specimens from MP demonstrated with homogenous cell distribution and cell cluster formation. In specimens from VMTS, cell cluster formation was predominant. We hypothesize that epiretinal cell proliferation may be initiated by localized vitreoretinal traction forming cell clusters that progress to homogenous cell multilayers at the vitreal side of the ILM after a period of time.

Immunocytochemical analysis demonstrated predominant staining for glial cell and hyalocyte marker such as GFAP, vimentin, CRALBP, CD45, and CD163. Myofibroblast-like cells with positive α-SMA expression were frequently found, whereas anti-cytokeratin, -Kir4.1, -CD34, -CD68, and -Ki67 were sparsely distributed in this series. Anti-neurofilament and -GAP43 were negative in all specimens tested. Anti-fibronectin, -laminin, and -collagen type IV were positive irrespective of the group of disease. Based on our results, we support the hypothesis that glial cells, notably retinal Müller cells, and hyalocytes are important components of epiretinal membranes in both MP and VMTS.

Most importantly, we found co-localizations of glial cell and hyalocyte marker and co-localization of anti-α-SMA with the hyalocyte marker anti-CD163. It appears that GFAP labeling in epiretinal cell proliferation needs to be reconsidered since positive GFAP labeling no longer allows for determination of cells to be of glial origin. Cells with double labeling for anti-GFAP and hyalocyte markers may represent hyalocytes. However, it is unknown if these 'hyalocytes' express GFAP endogenously or if they contain GFAP from other origin due to their well-known phagocyte activity. Another hypothesis is that double labeled cells may represent progenitor cells of transdifferentiated cells.

Co-localization of anti-CD163/α-SMA was seen in this study which supports the hypothesis that hyalocytes are able to transdifferentiate into myofibroblast-like cells in epiretinal membranes. Since positive α-SMA labeled epiretinal cells mainly presented in MP with incomplete PVD and VMTS, we hypothesize that the extent of PVD with persistent vitreoretinal adhesions may play an important role in differentiation of epiretinal cells and their antigen expression in eyes with MP and VMTS. Further investigation is needed to elucidate the influence of persistent vitreoretinal adhesions on behavior of hyalocyte cell populations, thereby addressing the role of cell transdifferentiation and the presence of progenitor cells in epiretinal membranes.

A.2 Zusammenfassung

Traktive Makulopathien wie die fortgeschrittene Form der epiretinalen Gliose, auch Macular pucker (MP) genannt, und das vitreomakuläre Traktionssyndrom (VMTS) entstehen an der vitreoretinalen Grenzfläche der Macula. Hauptkomponente der vitreoretinalen Grenzfläche ist die innere Grenzmembran, die Membrana limitans interna (ILM), die antero-posterior und tangential gerichtete Traktionen auf die Netzhaut überträgt. Diese mechanischen Zugkräfte entstehen durch persistierende Adhärenzen des Glaskörpers und durch epiretinale fibrozelluläre Membranen (ERM) an der vitrealen Seite der ILM. Die Entfernung von ILM und ERM ist daher wesentliches Ziel der vitreoretinalen Chirurgie bei MP und VMTS. Eine neue Präparationsmethode zur Aufbereitung von chirurgisch gewonnenen ILM-Präparaten bietet wichtige Vorteile gegenüber der konventionellen Einbettungs- und Schnittpräparation. Die neue Flachpräparation erlaubt die Darstellung des gesamten ILM-Präparates in seiner gesamten Größe mit vollständigem Zellbesatz.

Einhundertneunzehn ILM-Präparate wurden zusammen mit epiretinalem Gewebe während der Vitrektomie von 117 Patienten mit MP und VMTS gewonnen. Wir führten eine Flachpräparation mit Phasenkontrast- und Interferenzmikroskopie, LIVE/ DEAD ® Viabilitätsanalyse sowie indirekte immunzytochemische Färbungen mit 16 Antikörpern durch, die zellspezifisch gegen Gliazellen, Hyalozyten, retinale Pigmentepithelzellen und extrazelluläre Matrixkomponenten gerichtet waren. Insgesamt wurden die ILM-Präparate von 79 Augen mit MP und 40 Augen mit VMTS analysiert. Das Vorliegen einer kompletten oder inkompletten hinteren Glaskörperabhebung (PVD) wurde intraoperativ dokumentiert.

Die Viabilität zellulärer Proliferationen in Präparaten von MP mit kompletter PVD war signifikant höher als bei Präparaten von MP mit inkompletter PVD und VMTS. Während Präparate von MP eine homogene Zellverteilung als auch Zellclusterformationen zeigten, waren Zellcluster in Präparaten von VMTS häufiger. Persistierende Glaskörperadhärenzen mit vitreoretinaler Traktion, wie sie im Rahmen einer inkompletten PVD bestehen, könnten daher an der Ausbildung epiretinaler Zellcluster initial beteiligt sein und sowohl die Progression zellulärer Proliferationen als auch die Zellviabilität mitbestimmen.

Zellmarker für Gliazellen und Hyalozyten wie anti-GFAP, -Vimentin, -CRALBP, -CD45 und -CD163 prädominierten in allen Präparaten. Myofibroblasten-ähnliche Zellen mit positiver α-

SMA Färbung wurden ebenfalls häufig gefunden. Anti-Zytokeratin, -Kir4.1, -CD34, -CD68, and -Ki67 wurden selten positiv nachgewiesen. Anti-Neurofilament and -GAP43 wurden in unseren Präparaten nicht gesehen. Anti-Fibronectin, -Laminin, and -Kollagen Typ IV waren zumeist positiv unabhängig von der Grunderkrankung. Basierend auf unseren Ergebnissen gehen wir davon aus, dass Gliazellen, insbesondere retinale Müller Zellen, und Hyalozyten wichtige zelluläre Komponenten epiretinaler Membranen bei MP und VMTS darstellen.

Bedeutsam erscheint uns der Nachweis von Zellmarker-Doppelfärbungen. Co-Lokalisationen von Antikörpern spezifisch für Gliazellen und Hyalozyten wurden häufig gefunden, während die Co-Lokalisation von anti-α-SMA mit dem Hyalozytenmarker anti-CD163 selten auftrat. Wir gehen davon aus, dass die Interpretation positiver GFAP-Färbungen erneut überdacht werden sollte, da die alleinige positive Darstellung von anti-GFAP in immunzytochemischen Färbungen nicht länger als Grundlage für die Zuordnung von epiretinalen Zellen zu Populationen glialen Ursprungs dienen kann. Doppelfärbungen von anti-GFAP und Hyalozytenmarkern stellen vermutlich Hylozyten dar. Unklar bleibt jedoch, ob diese ‚Hyalozyten' GFAP endogen exprimieren oder ob sie GFAP extrazellulären Ursprungs enthalten als Zeichen ihrer phagozytären Aktivität. Eine weitere Hypothese ist, dass GFAP-positive ‚Hyalozyten' Progenitorzellen oder transdifferenzierte Zellen mit unbekannter Antigenexpression darstellen.

Über Doppelfärbungen von anti-α-SMA/CD163 in epiretinalen Membranen wurde bisher nicht berichtet. Unsere Ergebnisse stützen die Hypothese, dass Hyalozyten in Myofibroblasten-ähnliche Zellen transdifferenzieren. Da positive α-SMA gefärbte epiretinale Zellen vorwiegend in Präparaten von MP mit inkompletter PVD und VMTS gesehen wurden, gehen wir davon aus, dass persistierende vitreoretinale Adhärenzen eine wichtige Rolle bei der Differenzierung epiretinaler Zellen und ihrer Antigenexpression spielen. Weitere Untersuchungen müssen zeigen, ob und in welcher Weise vitreoretinale Traktionen das Verhalten von epiretinalen Zellen verändert. Dabei könnte insbesondere die Transdifferenzierung epiretinaler Zellproliferationen und das Vorkommen von Progenitorzellen in epiretinalen Membranen im Mittelpunkt stehen.

B. Abbreviations

BBG	Brilliant blue G
CD	cluster of differentiation
CRALBP	cellular retinaldehyde binding protein
DAPI	4’, 6-diamidino-2-phenylindole
ERM	epiretinal membrane
EthD-1	ethidium homodimer-1
GAP43	growth associated protein 43
GFAP	glial fibrillary acidic protein
ILM	internal limiting membrane
MB	Membrane blue
MP	macular pucker
NF	neurofilament
OCT	optical coherence tomography
PBS	phosphate buffered saline
PBTA	phosphate buffered triton azid
PPV	pars plana vitrectomy
PVD	posterior vitreous detachment
RMC	retinal Müller cell
RNFL	retinal nerve fiber layer
RPE	retinal pigment epithelium
SD	standard deviation
α-SMA	α-smooth muscle actin
SPSS	statistical package for the social science
TB	Trypan blue
VMTS	vitreomacular traction syndrome

1. Introduction

Progressive epiretinal gliosis, such as macular pucker (MP), and vitreomacular traction syndrome (VMTS) are traction vitreoretinopathies that develop at the vitreoretinal interface of the macular area. The major component of the vitreoretinal interface is the internal limiting membrane (ILM) that has attracted enormous interest for decades. The ILM is the site of epiretinal membrane formation and mediates tractional forces from the vitreous to retinal layers. There is general consent that vitreoretinal traction plays a crucial role in the pathogenesis and the clinical course of MP and VMTS. [Morris, 2000] Antero-posterior vitreoretinal traction is caused by persistent vitreoretinal adhesions due to an incomplete posterior vitreous detachment (PVD), whereas tangential traction is caused by contractive epiretinal membranes (ERMs) due to progressive fibrocellular proliferation at the vitreal side of the ILM. [Zarbin, 1990; Koerner, 1999; Gandorfer, 2005; Wylegala, 2006; Sebag, 2008]

Removal of the vitreous and epiretinal tissue is a principal goal of vitreoretinal surgery in MP and VMTS since epiretinal membranes represent the morphological correlate of typical symptoms found in these diseases, such as reduction of visual acuity and metamorphopsia. [Trese, 1983; Koerner, 1999] The concept of peeling off the ILM in eyes with traction maculopathies is supported by numerous studies reporting on improved functional and anatomic outcome. Furthermore, vitreoretinal surgery with ILM/ERM peeling was shown to minimize the recurrence rate of epiretinal cell proliferation. [Park, 2003; Kwok, 2004; Kwok, 2005; Tari, 2007] Therefore, ILM/ERM removal is a procedure widely accepted in the therapy of traction maculopathies.

By light and electron microscopic analysis, several studies characterized epiretinal cells and extracellular matrix components. According to their results, various cell types such as glial cells, hyalocytes, retinal pigment epithelial (RPE) cells, and fibroblast-like cells appear to be important in ERM formation. [Kampik, 1980; Gandorfer, 2002; Tari, 2007; Schumann, 2010] However, the specific role of epiretinal cell proliferation at the ILM in traction maculopathies is still a matter of debate. Even investigations of cell type specific antigen expressions of epiretinal cells did not allow for identifying the cells' origin exactly which is most probably caused by phenotypic transdifferentiation of epiretinal cells that adopt features of other cell types. To date, there is no specific marker of transdifferentiated cells [Vinores, 1990].

Recently, a new preparation method, the flat-mounted preparation of whole ILM/ERM specimens, was proposed to overcome limits of conventional serial sectioning preparation procedures. [Hisatomi, 2005; Hisatomi, 2006; Gandorfer, 2009; Liu, 2009] By preparing flat-mounted ILM specimens, the whole specimen can be visualized en-face, thereby detecting even small single cells on the ILM that would probably not be observed by conventional sectioning procedures. By using flat-mounted ILM/ERM specimens removed en-bloc during vitrectomy from eyes with MP and VMTS, the aim of our study was to obtain more accurate details on epiretinal cell proliferation with regard to cell distribution, cell viability, and cell immunoreactivity.

1.1 Anatomy of the vitreoretinal interface

The vitreoretinal interface (Figure 1.1), defined as morphological structure between the posterior vitreous cortex and the plasma membrane of retinal Müller cells (RMCs), consists of three components: (1) posterior vitreous cortex fibrils, (2) the ILM and (3) Müller cell footplates adjacent to the retinal side of the ILM. [Sebag, 1991; Gandorfer, 2004; Schumann, 2006; Schumann, 2007; Johnson, 2010]

1.1.1 Vitreous

The outer surface of the vitreous, the hyaloid membrane, is in contact with the posterior lens capsule, the zonular fibers, the pars plana epithelium, the retina, and the optic nerve head. The base of the vitreous maintains a firm attachment throughout life to the pars plana epithelium and the retina immediately behind the ora serrata. [Balazs, 1964; Ramesh, 2004] The vitreous composes of about 97% - 99% fluid. The remaining components are a mixture of collagen fibrils and hyaluronic acid, hyalocytes, inorganic salts and lipids that give the vitreous a gel-like form and consistency. [Scott, 1992] There are connections between vitreous collagen and the ILM. Vitreous collagen fibrils insert into the ILM, being most intense at the vitreous base and in some areas of the vitreous cortex. Recently, vitreous cortex was shown to be immunoreactive for collagen type II, V, IX and XI. [Sebag, 1992; Ponsioen, 2008]

1.1.2 Retinal Müller cells

Retinal Müller cells (RMCs) are the main type of glial cells in the retina that span the entire thickness of the retina and ensheath all retinal neurons. With retinal injury, RMCs are thought to become activated, to dedifferentiate and migrate from the retinal side to the vitreal side of the ILM where they proliferate and may drive epiretinal membrane formation. [Bringmann and Wiedemann, 2009] RMCs provide highly specialized physiological properties to support neurons in structure, nutrition and metabolism. Thus any impairment of supportive functions of them could cause and/or aggravate the dysfunction and loss of neurons. [Bringmann, 2006; Bringmann, 2009; Eberhardt, 2011] Vitreoretinal traction is considered to cause RMC activation. Activated Müller cells are known to upregulate the expression of glial fibrillary acidic protein (GFAP) that otherwise is not or very faintly expressed by RMC under normal conditions. [Lewis, 2003]

1.1.3 Internal limiting membrane

The internal limiting membrane (ILM), also termed basal lamina of the retina or internal limiting lamina, is an acellular structure that mainly composed of collagen type IV, VI and XVIII. [Heegaard, 1997; Ponsioen, 2008] It is thought to be the basement membrane of RMCs. The ILM typically shows a smooth vitreal side adjacent to the vitreous cortex and an undulated retinal side adjacent to RMC endfeet. The ILM is composed of three structures similar to other basement membranes: lamina fibroreticularis, lamina densa and lamina lucida. [Foos, 1972] The thickness of the ILM was found with regional difference in human adult eyes, being thickest at the macular region and thinnest at the ora serrata region. [Heegaard, 1997]

Figure 1.1

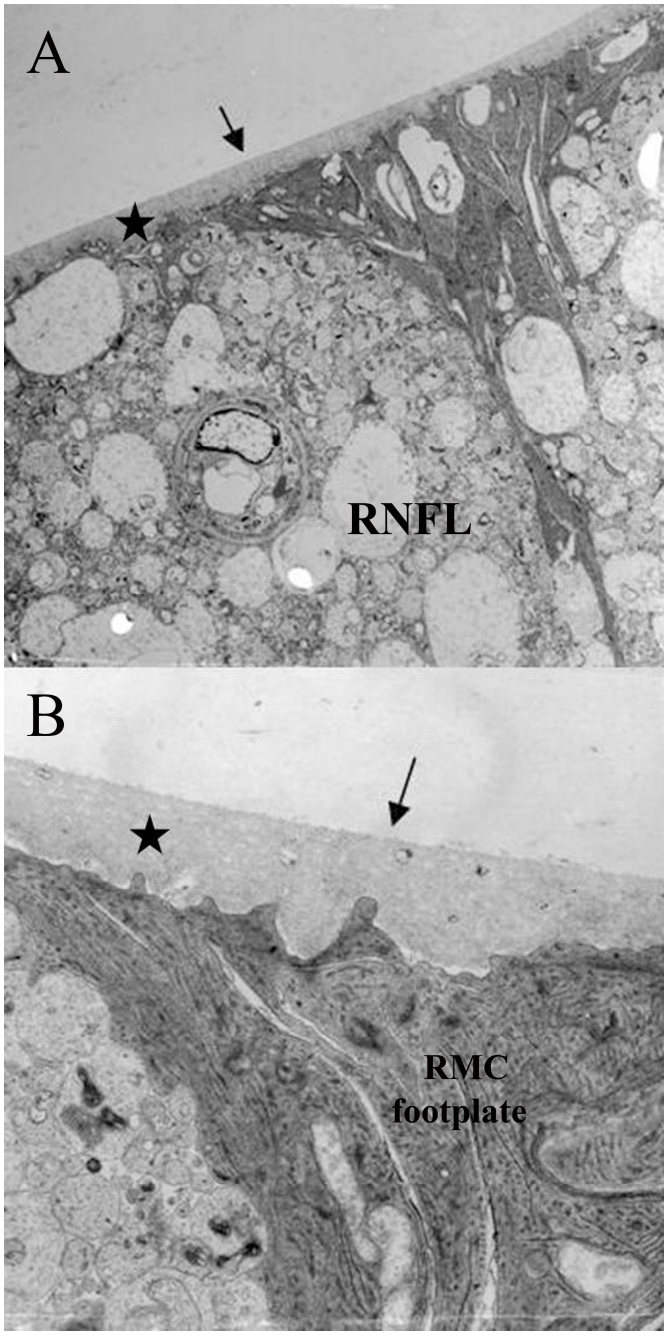

Figure 1.1 Transmission electron micrographs of the vitreoretinal interface and the retinal nerve fiber layer (RNFL) of the retina. The vitreal side (arrow) of the ILM (asterisk) is smooth, whereas the retinal side of the ILM presents with typical undulations corresponding to interdigitating processes of retinal Müller cell (RMC) footplates embedded in the RNFL. (Unpublished images of the Laboratory for Electron Microscopy, Department of Ophthalmology, Ludwig-Maximilians-University, Munich, by courtesy of Dr. med. R.G. Schumann.) (Original magnification: (A) x1, 800; (B) x9, 500)

1.2 Pathogenesis

1.2.1 Posterior vitreous detachment

Posterior vitreous detachment (PVD) is associated with (1) vitreous liquefaction and accumulation of fluid in the premacular portion of the vitreous cavity, and (2) incomplete or complete detachment of the posterior vitreous cortex from the ILM with varying degrees of persistent vitreoretinal adhesions. An anomalous PVD, called vitreoschisis, results from a split in the posterior vitreous cortex layers. As a consequence, residual vitreous collagen fibers are left behind at the vitreal side of the ILM and residual islands of cortical vitreous remain attached to the ILM following separation of the majority of vitreous gel from the surface of the retina. [Sebag, 2004; Sebag, 2008] Vitreoretinal traction of the retina caused by incomplete PVD may allow for activation and migration of glial cells from the inner retina to the surface of the ILM, where they are thought to proliferate and form epiretinal membranes. [Foos, 1978; Bringmann and Wiedemann, 2009]

Posterior vitreous detachment is associated with a variety of vitreoretinal pathologies, depending upon whether or not the posterior vitreous detachment is intact (full thickness) or split (partial thickness) which means complete or incomplete. [Sebag, 2008] Vitreoschisis was suggested to be pathogenic in MP. [Gupta, 2011] In VMTS, full-thickness vitreous cortex adherences to the macula with peripheral vitreoretinal separation induce vitreomacular traction. [Gandorfer, 2002; Sebag, 2008]

1.2.2 Macular pucker

Macular pucker (MP) (Figure 1.2) is a progressive form of epiretinal gliosis characterized by massive fibrocellular proliferation at the vitreal side of the ILM forming a dense, grayish-white appearing epiretinal membrane that causes severe tangential traction at the retina with retinal folding and distortion of retinal vessels. Retinal folds radiate in uni- or multi-directional fashion in the macular area, mostly towards the epicenter of the epiretinal membrane. Retinal traction can cause tortuosity of the perimacular vessels, macular edema, and intraretinal bleeding. According to density and contractility of epiretinal cell proliferation, milder forms of epiretinal gliosis are defined as cellophane maculopathy and surface wrinkling maculopathy referring to a thin, glistening membrane with or without superficial

retinal folds. Epiretinal membranes are a common finding in older patients that mostly occur in the absence of any ocular pathology. However, epiretinal gliosis may be associated with other ocular disorders and after intraocular surgery. [Cox, 1995; Jacobsen, 1996; Jahn, 1999; Katira, 2008] In MP, patients usually complain of severe vision loss and metamorphopsia. [Dellaporta, 1973; Tari, 2007] Bowing and blurring when looking at lines on chart paper (Amsler grid) are noticed by patients with retinal folding in the vitreous area. Retinal imaging technique such as optical coherence tomography (OCT), fundus photography and fluorescein angiography are used to enhance accuracy of MP diagnosis. [Sebag, 2007]

1.2.3 Vitreomacular traction syndrome

Vitreomacular traction syndrome (VMTS) (Figure1.3) is a vitreomacular disorder characterized by a firm and persistent vitreoretinal adhesion in eyes with an incomplete PVD. The vitreous is detached in the periphery whereas the vitreous remains attached to the macula and the optic nerve head, thereby causing vitreoretinal traction with macular edema and peripapillary edema that may progress to cystoid retinal degeneration. Patients complain of moderate to severe loss of vision and metamorphopsia. [McDonald, 1994; Figus, 2008] Incomplete PVD varies from peripheral vitreous separation with residual foveal attachment to multiple areas of detachment with focal posterior and peripheral vitreous attachment. Once thought to be a rare distinct clinical entity, VMTS is now considered a spectrum of macular diseases. [Shechtman, 2009] Although the clinicopathologic correlation with different features of VMTS has not been determined yet, the predominance of myofibroblasts was reported that may induce the progressive VMTS characteristic in this disorder. [Shinoda, 2000; Gandorfer, 2002]

Figure 1.2 Macular pucker

Figure 1.3 Vitreomacular traction syndrome

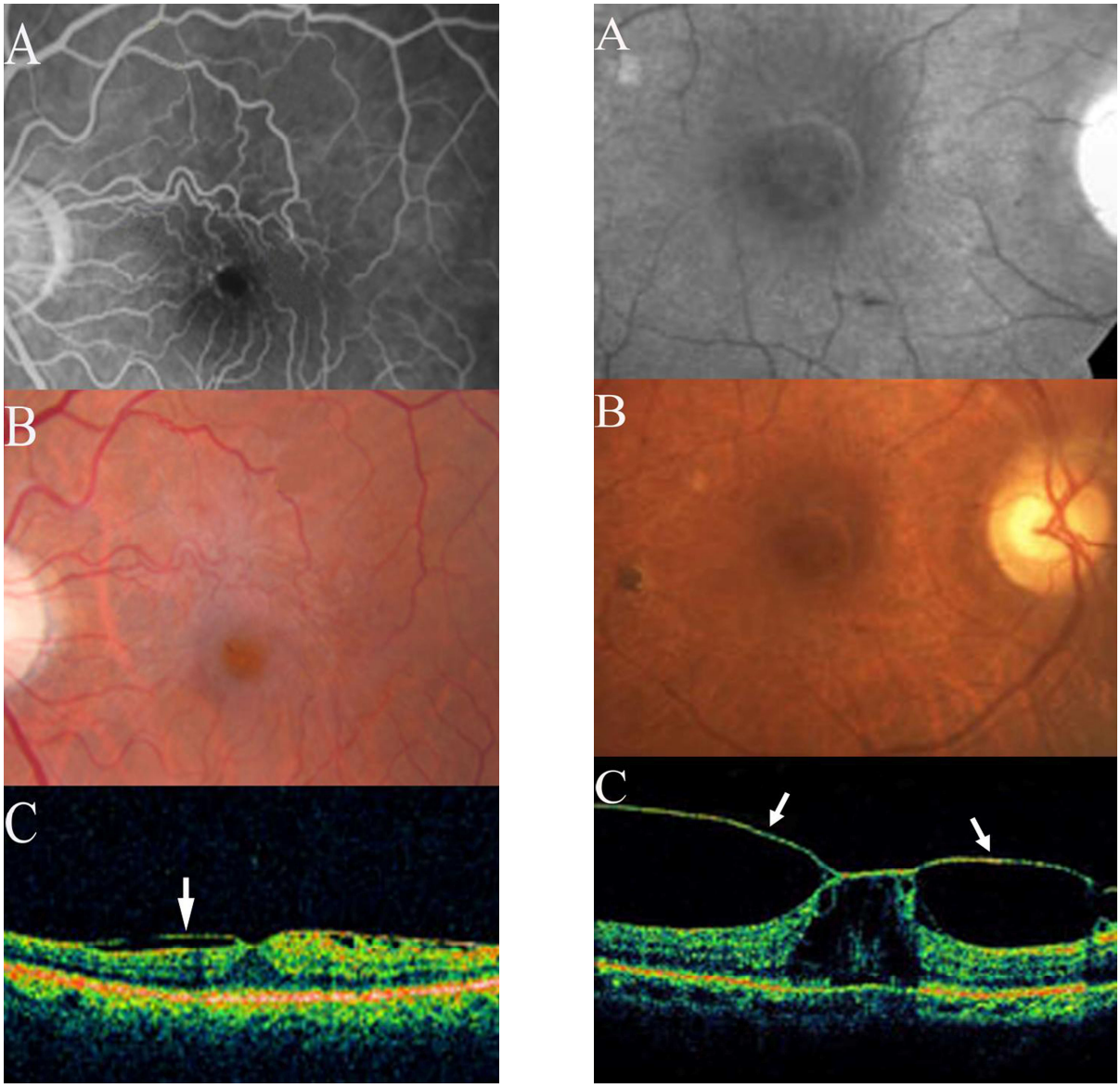

Figure 1.2 and 1.3 Retinal imaging of eyes with MP and VMTS. (A) Fluorescein angiography and (B) fundus photography show retinal vessel tortuosity in MP and VMTS. (C) OCT images demonstrate the presence of the ERMs and vitreomacular traction (arrows) in MP and VMTS. (Photographs by courtesy of the Department of Ophthalmology, Ludwig-Maximilians-University, Munich)

1.3 Cells implicated in the pathogenesis of vitreoretinal maculopathies

Morphological analyses of surgically excised ILM specimens have demonstrated a variety of cells in epiretinal membranes of idiopathic vitreoretinal maculopathies that are thought to be of retinal and extra-retinal origin including glial cells (Müller cells, astrocytes, and microglia), retinal pigment epithelial cells, hyalocytes, fibrocytes and myofibroblasts. [Kampik, 1981; Smiddy, 1989; Gandorfer, 2005; Schumann, 2006]

1.3.1 Retinal glial cells

Retinal glial cells included macroglia (RMCs and astrocytes) and microglia. Retinal Müller cells are the main type of glial cells in the retina, which have been introduced above in 1.1.2.

Astrocytes are a sub-type of glial cells in the retina. They are also known as astrocytic glial cells. They possess a star shape with numerous processes enveloping synapses of neurons. They migrate into the retina via the optic nerve during embryogenesis, and are located exclusively in the inner layers of the retina. [Watanabe, 1988; Sandercoe, 1999] Like Müller cells, astrocytes are also considered to dedifferentiate, proliferate, and migrate from the retinal side to the vitreous side of the ILM where they may participate in ERM formation. [Ramírez, 1996] Immunohistochemical findings suggested that astrocytes also express GFAP similar to activated RMCs in ERMs. [Sandercoe, 1999]

Microglial cells account for approximately 20% of the total glial cell population in the central nervous system. They belong to the mononuclear phagocyte system and constitute the population of resident macrophages in the brain and the retina. Activated microglia cells become immunocompetent and are MHC (major histocompatibility complex) class 1 and class 2 positive. [Kreutzberg, 1995; Huang, 2008] Microglia activation is associated with CD68 (cluster of differentiation 68) immunoreactivity. [Wang, 2010] In response to injury, microglia cells undergo rapid activation and produce both proinflammatory and regenerative neurotrophic factors. [Ng, 2009; Ibrahim, 2011]

Recent years increasing effort focused in assessing the plasticity of glial cells as a potential source for new neurons in the injured eye. Following injury, RMCs are proposed to differentiate and acquire stem or precursor cell like properties. [Bringmann, 2009; Berninger, 2010]

1.3.2 Retinal pigment epithelial cells

Retinal pigment epithelial (RPE) cells are multifunctional pluripotent cells that are characterized by intracytoplasmic melanin granules, microvilli and junctional complexes. RPE cells have various functions. Most importantly, they participate in cell metabolism of photoreceptors, and they are related to vitamin A metabolism and regeneration in the visual cycle. Retinal pigment epithelium cells are capable of phagocytosis. [Uchida, 2005; Strauss, 2009] Additionally, they are proposed to possess immunosuppressive properties. [Sugita, 2009; Sugita, 2010]

1.3.3 Hyalocytes

Hyalocytes, first described in 1845 by Hannover and then named by Balazs, are resident cells distributed in the vitreous cortex situated 20 – 50 µm apart from the ILM. [Hannover, 1845; Balazs, 1964; Sebag, 1992] Hyalocytes most probably derive from the monocytes-macrophage lineage, and appear to be involved in the pathogenesis of various vitreoretinal diseases. They are thought to mediate ERM contractility. [Hirayama, 2004; Kohno, 2009] Other origins have also been proposed such as derivations from neuroglia of the retina, from mesenchymal cells of the retinal vasculature, and from cells of the hyaloid system. [Sebag, 1992] Hyalocytes were shown to express the leukocyte-associated antigens CD45, CD64 and ED2 (CD163). [Lazarus, 1994; Zhu, 1999; Sakamoto, 2003; Qiao, 2005]

1.3.4 Myofibroblasts

Myofibroblasts are found subepithelially in many mucosal surfaces. They are known to participate in wound-healing, inflammation or fibrosis of non-neoplastic conditions, and in tumor growth. Myofibroblasts are of spindled or satellite morphology and share features with fibroblasts in Golgi apparatus and expression of smooth muscle actin. However, they are devoid of lamina-α structures seen in smooth muscle cells [Eyden, 2001; Eyden, 2009]. Myofibroblasts were reported to be present or even predominant in the vitreoretinal disorders

such as MP and VMTS. Their immunophenotype is characterized by α-smooth muscle actin (α-SMA). [Gandorfer, 2002; Ina, 2011]

1.3.5 Macrophages

Macrophages are white blood cells deriving from differentiation of monocytes in tissues. Macrophages function in non-specific defense (innate immunity) as well as in specific defense mechanisms (adaptive immunity) of vertebrate animals. They stimulate lymphocytes and other immune cells to respond to pathogens. [Streit, 2001] Macrophages express of the cell type associated antigen CD68. However, to date there is no specific marker to differentiate between macrophages and microglial cells. [Bosman, 1999; Khazen, 2005]

1.4 Surgical Treatment

1.4.1 Pars plana vitrectomy

Pars plana vitrectomy (PPV) is generally agreed to be the most appropriate treatment for vitreoretinal disorders. In early 1970s, the original purpose of vitrectomy was to remove clouded vitreous. In 1991, Kelly and Wendel introduced PPV to close macular holes. Meanwhile the removal of the ILM during vitrectomy is recommended in most vitreomacular diseases. Numerous studies have approved that vitrectomy improves visual acuity in at least 70% of individuals with MP and VMTS [Kelly, 1991; Koerner, 1999].

1.4.2 Vital dyes in vitreoretinal surgery

Vital dyes help to visualize translucent structures such as the ILM and ERM in vitreoretinal surgery, and therefore, they facilitate ILM removal. Recently, this technique was named ‘chromovitrectomy’ [Rodrigues, 2005]. Brilliant Blue G (BBG) was suggested to stain the ILM safely. Other dyes, such as Trypan Blue (TB) or Membrane Blue (MB) were introduced to stain epiretinal tissue providing only a weak contrast of the ILM. [Enaida, 2006; Haritoglou, 2008; Schumann, 2010]

1.5 Immunomarker mentioned in this study

1.5.1 CD163

CD163, also called ED2, recognizes membrane and cytoplasmic antigens of tissue macrophages, discriminating between distinct subpopulations of macrophages/monocytes. [Yang, 2002] Immunofluorescent analysis of rat eyes showed that 90% of hyalocytes were positive for ED2 [Sakamoto, 2003].

1.5.2 CD45

CD45, also known as protein tyrosine phosphates (PTPRC), is an enzyme that was originally called leukocyte common antigen in hematopoietic cells. It is expressed among hematopoietic cells, and is also expressed constitutively in hyalocytes and microglia. [Kaplan, 1990; Lazarus, 1994; Zhu, 1999]

1.5.3 Glial fibrillary acidic protein

Glial fibrillary acidic protein (GFAP) is an intermediate filament protein that was thought to be specific for glial cells in the past. It is closely related to its non-epithelial family member's vimentin, desmin, and peripherin, which are all involved in the structure and function of the cell's cytoskeleton. The up-regulation of GFAP is the most sensitive response of Müller cells to retinal injury, and can be used as marker for Müller cell activation. Its exact function remains poorly understood. [Guérin, 1990; Bongcam-Rudloff, 1991; Lewis, 2003; Lesnik Oberstein, 2008; Middeldorp, 2011]

1.5.4 Vimentin

Vimentin is a member of the intermediate filament family of proteins that is especially found in connective tissue. Intermediate filaments are an important structural feature of eukaryotic cells. Along with microtubules and actin microfilaments, they generate the cytoskeleton. Although most intermediate filaments are stable structures, in fibroblasts vimentin exists as a dynamic structure. This filament protein is used as a marker for mesodermally derived cells, such as retinal glial cells, fibroblasts, endothelial cells, lymphoid cells and melanocytes. [Fuchs, 1994; Lesnik Oberstein, 2008; Bhatia, 2009; Semple-Rowland, 2010]

1.5.5 Cellular retinaldehyde binding protein

Cellular retinaldehyde binding protein (CRALBP) is encoded by the retinaldehyde binding protein (RLBP1) gene in humans. It is a functional component of the visual cycle. This gene was found in RPE cells and Müller cells of the neuroretina. [Maw, 1997; Limb, 2002; Walcott, 2003; Collery, 2008]

1.5.6 Kir4.1

Kir4.1 may form a heterodimer with another potassium channel protein and may be responsible for the potassium buffering action of glial cells in the brain. Retinal Müller glial cells, astrocytes, RPE cells may be able to be distinguished by diminished presence of the integral membrane protein Kir4.1. [Connors, 2006; Hu, 2010] Kir4.1 is found on RMCs endfeet membranes and is involved in inhibition of glial cell growth. [Higashimori, 2007; Ruiz-Ederra, 2007]

1.5.7 α-Smooth muscle actin

Alpha-smooth muscle actin (α-SMA) is one of six different actin isoforms that have been identified. Actins are highly conserved proteins that are involved in cell motility, structure and integrity of cells. Its expression is associated with the presence of myofibroblasts, epithelial cells, striated muscle cells and myocardium. [Harris, 1992]

1.5.8 Cytokeratin

Cytokeratins (CKs) are proteins of keratin-containing intermediate filaments found in the intracytoplasmic cytoskeleton of epithelial tissue. [Franke, 1979] For detecting cytokeratins, pan-cytokeratin antibody with the clone designation C11 is frequently used as the marker of RPE cells [Fuchs, 1991; Boyd, 2009].

1.5.9 Growth associated protein 43

Growth associated protein 43 (GAP43) is considered as a crucial component of the axon and presynaptic terminal. This protein is abundant during development but absent in normal retina. It is used to identify neuronal growth cones during development and axonal regeneration. In

the retina, GAP43 is involved in synapse formation. Ganglion cells show an elevated expression of GAP43 after ischemia-inflicted damage. [Fisher, 2005; Dijk, 2007; Kusik, 2010]

1.5.10 Neurofilament

Neurofilament (NF) is the 10 nm intermediate filaments found specifically in neurons. The subunits of neurofilament protein are related structurally to intermediate filaments of other tissues such as the keratin subunits in epithelia. The level of neurofilament gene expression seems to be directly related to the neurons (axons) of the central and peripheral nervous system, and may be a useful tool for the identification of ganglion cells and bipolar cells. [Lesnik Oberstein, 2008]

1.5.11 CD34

CD34 molecule is a cell surface glycoprotein and functions as a cell-cell adhesion factor. It may also mediate the attachment of stem cells to bone marrow extracellular matrix or directly to stromal cells. It is expressed on the surface of lymphohematopoietic cells, stem and progenitor cells, small vessel endothelial cells and embryonic fibroblasts. [Simmons, 1992; Satterthwaite, 1992; Sandercoe, 1999]

1.5.12 CD68

CD68 is a glycoprotein which binds to low density lipoprotein. It is expressed in monocytes/macrophages. [Holness, 1993; Manduch, 2009] Activated microglia cells also express the CD68 antigen. [Yang, 2000; Wang, 2010] To date, there is no specific marker to differentiate between macrophages and microglia.

1.5.13 Collagen IV

Type IV collagen is a type of collagen found primarily in the basal lamina. It lacks the regular glycine in every third residue necessary for the tight collagen helix. This makes the overall arrangement sloppier with kinks that cause the collagen to form a sheet. [Khoshnoodi, 2008]

1.5.14 Fibronectin

Fibronectin (FN) is a high-molecular weight extracellular matrix glycoprotein that binds to membrane-spanning receptor proteins called integrins. In addition to integrins, it also binds extracellular matrix components such as collagen, fibrin and heparan sulfate proteoglycans. Fibronectin plays a major role in cell adhesion, cell growth, migration and differentiation, and it is important for wound healing. Fibronectin immunoreactivity can be found in retinal vessels. [Hiscott, 1992; Roy, 1996; Pankov, 2002; Chen, 2009]

1.5.15 Laminin

Laminins are major proteins in the basal lamina, a protein network foundation for most cells and organs. They are an important and biologically active part of the basal lamina, influencing cell differentiation, migration, adhesion, and cell survival. Studies showed that human ERMs from patients of varying durations were immunoreactive for laminin. [Timpl, 1979; Lesnik Oberstein, 2008; Chen, 2009]

1.5.16 Ki67

Antigen Ki67 is a nuclear protein that is associated with cellular proliferation. It is an excellent marker to determine the growth fraction of a given cell population since it is expressed in proliferating cells. Studies showed that Ki67-positive proliferating cells were present in undifferentiated retina, but not in differentiated retina. [Schonk, 1989; Heidenkummer, 1992; Walcott, 2003]

Table 1.1 Correlation of antibodies used in this study and immunospecificity

Immunomarker	Immunospecificity
CD163	hyalocytes
CD45	hyalocytes, microglia
GFAP	glial cells (Müller cells, astrocytes)
Vimentin	glial cells
CRALBP	Müller cells, retinal pigment epithelial cells
Kir4.1	glial cells
α-SMA	myofibroblasts, epithelial cells
Cytokeratin	retinal pigment epithelial cells
GAP43	axonal regeneration, regenerated ganglion cells
Neurofilament	retinal ganglion cells and bipolar cells
CD34	endothelial cells, stem cells
CD68	macrophages, microglia, monocytes
Collagen IV	internal limiting membrane
Fibronectin	cell adhesion, migration, differentiation
Laminin	cell adhesion, migration, differentiation
Ki67	cell proliferation

2. Material and Methods

2.1 Laboratory equipment

(1) Refrigerator

(BOSCH, Germany)

(2) Incubator

(Memermt, Schwabach, Germany)

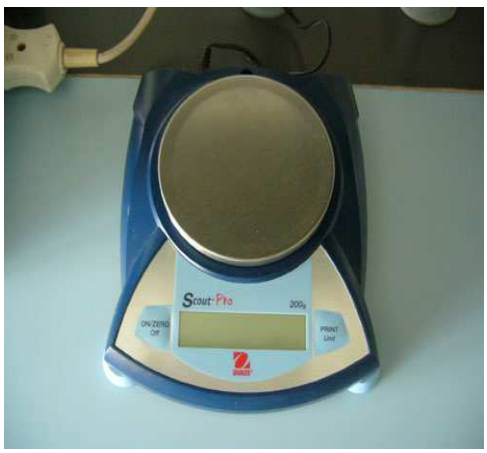

(3) Electronic balance scout pro SPU 202

(Ohaus, Pine Brook, NJ USA)

(4) Shaker IKA-VIBRAZ-VXR

(IKA, Staufen, Germany)

(5) Fluorescence microscope LEICA MS5
(Leica, Wetzlar, Germany)

(6) Captair® chem Filtair
(erlab, Köln, Germany)

(7) Light microscope Leica DM2500
(Leica, Wetzlar, Germany)

2.2 Reagents

Aqua dest.	(Braun 6724092)
0.5% BSA	(SIGMA A-9647, Taufkirchen, Germany)
Donkey Cy2	(Dianova, Hamburg, Germany)
Donkey Cy3	(Dianova, Hamburg, Germany)
Donkey Cy5	(Dianova, Hamburg, Germany)
Donkey serum	(Dianova, Hamburg, Germany)
ImmnunoSelect® Antifading Mounting Medium DAPI	(Dianova AKS-38448, Hamburg, Germany)
LIVE/ DEAD ® Viability/ Cytotoxicity Kit * for mammalian cells *	(Molecular Probes L-3224, Invitrogen, Carlsbad, USA)
3.4% NaCl	(Pharmacy of Ludwig-Maxmilians University, N18)
Na_2HPO_4	(MERCK 1.06346, Darmstadt, Germany)
$Na_2H_2PO_4$	(MERCK 1.06580, Darmstadt, Germany)
0.1% Na-Azid	(SIGMA S-8032, Taufkirchen, Germany)
Paraformaldehyd	(MERCK 1.04005, Darmstadt, Germany)
Pepsin	(Sigma-Aldrich P7000, Taufkirchen, Germany)
PBS Buffer	(Pharmacy of Ludwig-Maxmilians University, G09)
0.1% Triton X-100	(SIGMA X-100, Taufkirchen, Germany)

2.3 Prescriptions

2.3.1 Phosphate buffered saline (PBS) 0.1M

$Na_2HPO_4 – 2H_2O$	14.42g
$Na_2H_2PO_4 – H_2O$	2.62g
Distilled water	1000 ml
Adjust to PH 7.4 with HCl	

2.3.2 Paraformaldehyde (PFA)

Paraformaldehyde	2g
0.1M PBS	50ml
80°C heat for 15 min	
Place in the 4°C refrigerator	

2.3.3 Enzyme

10% Pepsin	1000µl
0.1M PBS	1ml
Place in the -20°C refrigerator	

2.3.4 Phosphate buffered triton azid (PBTA)

0.1 M PBS (Ph7.4)	100ml
0.5% BSA	500µg
0.1% Triton X-100	100 µl
0.1% Na-Azid	100mg
Place in the -20°C refrigerator	

2.4 Antibodies

CD163	(SantaCruz sc-58965, Heidelberg, Germany)
CD45	(SantaCruz sc-1123, Heidelberg, Germany)
GFAP	(DAKO Z0334, Glostrup, Denmark)
vimentin	(DAKO M0725, Glostrup, Denmark)
CRALBP	(SantaCruz sc-18757, Heidelberg, Germany)
Kir4.1	(SantaCruz sc-23637, Heidelberg, Germany)
α-SMA	(SIGMA C6198, Taufkirchen, Germany; SantaCruz sc-130617, Heidelberg, Germany)
pan- cytokeratin	(Sigma C2562, Taufkirchen, Germany)
GAP43	(SantaCruz sc-7457, Heidelberg, Germany)
neurofilament	(DAKO M0762, Glostrup, Denmark)
CD34	(SantaCruz sc-19621, Heidelberg, Germany)
CD68	(SantaCruz sc-7082, Heidelberg, Germany)
collagenIV	(SantaCruz sc-11360, Heidelberg, Germany)
fibronectin	(DAKO A0245, Glostrup, Denmark)
laminin	(DAKO Z 0097, Glostrup, Denmark)
Ki67	(SantaCruz sc-7844, Heidelberg, Germany)

2.5 Materials

This is a series of 119 surgical specimens obtained during vitrectomy for idiopathic MP and idiopathic VMTS between January 2008 and April 2010. The specimens consisted of the ILM and epimacular tissue, and were removed en-bloc from 119 eyes of 117 patients including 79 eyes with MP and 40 eyes with VMTS. Intraoperatively, the state of the vitreous was assessed. Regarding the presence of PVD, we divided all specimens from eyes with MP into 2 groups: (1) 39 specimens were removed from eyes with MP and complete PVD; and (2) 40 specimens were removed from eyes with MP and incomplete PVD.

All 119 specimens were processed for phase contrast microscopy, interference microscopy and cell nuclei staining. LIVE/ DEAD ® cell viability assay was performed in 27 specimens from 27 patients including 10 eyes with MP and complete PVD, 9 eyes with MP and incomplete PVD, and 8 eyes with VMTS. For immunocytochemistry, 51 flat-mounted ILM specimens from 51 patients were processed including 16 eyes with MP and complete PVD, 16 eyes with MP and incomplete PVD, and 19 eyes with VMTS. The remaining 40 specimens from 38 patients were only processed for phase contrast microscopy, interference microscopy and cell nuclei staining as mentioned above, because these specimens showed multiply folded during flat-mounted preparation appearing not suitable for immunolabeling procedures. (Table 2.1)

The surgical procedure consisted of a three-port pars plana vitrectomy with en-bloc peeling of the ILM and the ERM. All patients were operated by experienced surgeons at the University Eye Hospital Munich. Forty-seven patients underwent a combined procedure of vitrectomy and cataract extraction. Only specimens presenting the ILM were included. Approval from the Institutional Review Board was obtained as well as the Informed Consent from each patient.

Table 2.1 Number of specimens processed by different methods

Test	MP with complete PVD (n=39)	MP with incomplete PVD (n=40)	VMTS (n=40)
Phase contrast / interference microscopy	39	40	40
Cell staining by DAPI	39	40	40
LIVE/ DEAD ® cell viability assay	10	9	8
Immunocytochemical analysis	16	16	19

The surgical procedure of a three-port pars plana vitrectomy was performed as followed. Before opening the infusion line, the status of the posterior hyaloid was determined using a plano-concave contact lens. If the vitreous was partially attached to the retina, PVD was induced by suction with the vitrectomy probe over the optic disk. The posterior hyaloid was detached from the retina and excised up to the periphery. Then, peeling the ILM was performed using an end-gripping Eckardt forceps. To improve the precision of ILM peeling and to avoid incomplete removal, vital dyes had been applied during surgery: (1) BBG (0.5 ml, 0.25%, Brilliant Peel®; Fluoron® GmbH, Neu-Ulm, Germany) was used to stain 20 specimens from MP with complete PVD, 23 specimens from MP with incomplete PVD and 26 specimens from VMTS; (2) MB (0.5ml, 0.15%, DORC, Dutch Ophthalmic Research Center Zuidland, the Netherlands) was used to stain 2 specimens from MP with complete PVD and 1 specimen from VMTS; (3) TB (0.5ml, 0.15%, DORC, Dutch Ophthalmic Research Center Zuidland, the Netherlands) was used only in 1 specimen from VMTS. Overall, vital dyes were administered in 73 eyes to visualize the ILM. In the remaining 46 eyes, no intravitreal dye was used. In case of coexisting cataract, a combined procedure was performed. The ILM with epimacular tissue was harvested and processed for our study.

The patients' records were reviewed for age, gender, previous ocular surgery and preoperative history such as trauma. Additional information such as duration of symptoms was evaluated if available.

2.6 Methods

2.6.1 Specimen fixation and flat-mounted preparation

After removal, the excised tissue was immediately placed into a mixture of PFA for at least 24 hours. Then, specimens were extended onto glass slides as whole mounted membranes to show their maximum area by using fine-tipped forceps under a light microscope (Leica DM2500; Leica, Wetzlar, Germany).

2.6.2 LIVE/ DEAD ® viability assay

The LIVE/ DEAD ® Viability/ Cytotoxicity Kit (Invitrogen, Carlsbad, CA, USA) for mammalian cells test is to provide a two-color fluorescence cell viability assay. The polyanionic dye calcerin AM is well retained within all cells, producing an intense uniform green fluorescence in all cells (ex/em -495nm/ -515nm). Ethidium homodimer-1(EthD-1) is a high-affinity nuclei acid stain that is weakly fluorescent until bound to DNA emitting red fluorescence. As cell-impermeant viability indicator, EthD-1 can produce a bright red fluorescence in dead cells (ex/em -495nm/ -630nm), whereas it is excluded by the intact plasma membrane of live cells. This assay has been already proved to be used to determine the percentage of dead and live cells. [Ammar, 2010]

Due to the fluorescence microscope of our laboratory, in our study all cells were stained with blue color by calcerin AM, whereas dead cells were shown with red color by binding EthD-1. Based on the time of fixation in PFA, we had 2 groups in this assay: 21 specimens were immediately processed after surgical removal; and 6 specimens were processed 24 hours after surgical removal.

After preparing ILM specimens as flat-mounted membranes, one drop (almost 100µl) of LIVE / DEAD ® reagent was added. Then specimens were incubated for 30 minutes, and a coverslip was mounted on glass slides. The fluorescence microscope Leica (Leica MS5; Leica, Wetzlar, Germany) was used for analysis at magnifications between x50 and x400.

2.6.3 Phase contrast and interference microscopy

In phase contrast microscopy, differences in image contrast are produced by using an optical mechanism to translate subtle variations in phase into corresponding changes in amplitude [Lee, 2011]. Interference microscopy was applied to detect changes in surface height, such as cellular proliferation compared to bare ILM [Gandorfer, 2009]. Differences in image intensity are produced by splitting the entering light into two beams that pass through the specimen and become recombined in the image plane, where the interference effects make the transparent object details become visible [Duncan, 2011].

All 119 flat-mounted specimens were labeled with DAPI for cell nuclei staining. Specimens were analyzed using a modified fluorescence microscope (Leica MS5; Leica, Wetzlar, Germany) that enabled us to perform both interference and phase contrast microscopy at magnifications between x50 and x400.

2.6.4 Immunocytochemistry

After PFA fixation, the ILM specimens were rinsed with 0.1M PBS (pH7.4) 2 times for 5 minutes and incubated with the pepsin for 30 minutes at room temperature. Then specimens were rinsed with 0.1M PBS again 2 times for 5 minutes. The samples were blocked using normal donkey serum (dilution, 1: 20) in PBTA for 2 hours at room temperature. Afterward, they were rinsed with PBTA 3 times for 5 minutes and then incubated with primary antibodies (anti-CD34, -CD45, -CD68, -CD163, -collagen IV, -CRALBP, -pan-cytokeratin, -fibronectin, -GFAP, -GAP43, -Ki67, -Kir4.1, -laminin, -NF, -vimentin) according to manufacturer's instructions for 24 hours at the incubator (37°C). Since the maximum number of fluochromes used at one time was limited, and the antibody combinations were limited caused by the species they were originating from, we only used combinations of 3 antibodies.

The membranes were rinsed with PBTA for 3 times and incubated with the secondary antibodies (anti- α-SMA, cy2, cy3, cy5) according to manufacturer's instructions for 2 hours at room temperature. Then specimens were rinsed with PBTA 4 times for 10 minutes and with PBS 3 times for 5 minutes. As mentioned above, we used the combination of 3 antibodies.

Finally, the specimens were prepared as flat-mounted membranes. One drop of antifading mounting medium DAPI was added. Then, specimens were placed onto the Crystal/ Moune

(Biomedia, California) with coverslip and viewed under the fluorescence microscope at magnifications between x50 and x400.

For control specimens, primary antibodies were substituted with diluent followed by incubation with secondary antibodies alone. All other procedures were identical to normal immunolabeling procedures.

2.7 Statistical analysis and photodocumentation

Images, captured by a digital camera (ProgRes CF; Jenoptik, Jena, Germany), were analyzed measuring the specimen area in consideration of magnification by Adobe Photoshop CS4. Cell quantification was analyzed using ImageJ software, a Java-based image processing program developed at the National Institutes of Health [Gering, 2004]. The dead cell and total cell count were calculated by ImageJ. If the total cell count was less than 100, labeled nuclei were counted in fluorescence micrographs using ImageJ software with manual counting. If the total cell count was over 100, we used automatic counting. Finally, measured areas and cell counts of specimen parts were added up from each patient.

Statistical analysis of total cell counts and total area of specimens was performed using the computer software, Statistical Package for the Social Science (SPSS) version 16.0. Mann-Whitney Test, Kruskal-Wallis-Test and Chi-Square Test were performed for evaluation. $P < 0.05$ was considered to be statistically significant.

3. Results

3.1 Clinical features

Fifty-nine women and 58 men were included in this series, corresponding to 71 right eyes and 48 left eyes. Two male patients underwent surgery on both eyes. The total of 119 specimens was divided into three groups: (1) specimens removed from eyes with MP and complete PVD (n = 39), (2) specimens removed from eyes with MP and incomplete PVD (n = 40), and (3) specimens removed from eyes with VMTS (n = 40). The state of the vitreous was intraoperatively confirmed during surgery.

The average age at time of surgery was 69.3 years (ranged from 41 to 81 years), and the age distribution of patients was similar in all three groups of diagnosis. With regard to previous ocular surgery, 27 eyes had undergone cataract surgery with phacoemulsification and implantation of an intraocular lens, including 6 eyes with MP and complete PVD, 10 eyes with MP and incomplete PVD and 11 eyes with VMTS. The duration of symptoms according to the patients' documents ranged from 3 weeks to more than 5 years.

Among all 119 specimens, 73 samples were removed after administration of vital dyes into the vitreous cavity: BBG was used to stain 20 specimens from MP with complete PVD, 23 specimens from MP with incomplete PVD and 26 specimens from VMTS; MB was used to stain 2 specimens from MP with complete PVD and 1 specimen from VMTS; TB was used only in 1 specimen from VMTS, which was already mentioned above in section 2.5.

3.2 LIVE/ DEAD ® cell viability assay

3.2.1 General features

LIVE/ DEAD ® assay evaluation focused on a consecutive series of 27 specimens obtained during vitrectomy. In detail, 10 specimens from eyes with MP and complete PVD, 9 specimens from eyes with MP and incomplete PVD, and 8 specimens from eyes with VMTS were tested. The distribution of patients' age and gender involved in this series is shown in Table 3.1. Figure 3.1 presents dead cells as red cell nuclei and the amount of total cells as blue cell nuclei.

The viability percentage showed a broad variety from 18% to 98% with a mean of 76.6% (standard deviation, SD 27.8%). The mean cell viability percentages were 94.5% (SD 4.8%) in specimens removed from eyes with MP and complete PVD, 56.4% (SD 28.9%) in specimens removed from eyes with MP and incomplete PVD, and 64.8% (SD 25.9%) in specimens removed from eyes with VMTS. We found significantly more viable cells in specimens from MP than in specimens from VMTS ($p = 0.012$, Mann-Whitney Test). Comparing specimens of MP with complete and incomplete PVD, there was a significant higher viability in specimens from eyes with MP and complete PVD ($p = 0.014$, Mann-Whitney Test).

Six specimens (including one specimen from MP with complete PVD, three specimens from MP with incomplete PVD and two specimens from VMTS) were tested 24 hours after surgical removal with meanwhile storage in BSS at +4°C. These specimens were found with a mean viability percentage of 83% (SD 28%), which ranged from 32% to 98%.

Table 3.1 LIVE/ DEAD ® viability assay and clinical data

Case	Gender	Age	Eye	Diagnosis	Dye	Area (mm^2)	Total cells	Live / Dead cell	Viability (%)
1	M	80	R	MP-1	BBG	2.9	55	50/5	91
2	M	74	R	MP-1	-	5.5	1719	1418/3041	82
3	F	68	R	MP-1	-	5.0	841	810/31	96
4	M	72	R	MP-1	-	3.6	1734	1686/48	97
5	M	81	R	MP-1	BBG	2.4	663	632/31	96
6	M	60	R	MP-1	-	5.4	1018	906/110	89
7	M	71	L	MP-1	BBG	16.3	6595	6298/297	95
8*	M	71	R	MP-1	-	3.4	193	185/8	96
9	F	70	R	MP-1	-	26.9	7459	7174/285	96
10	F	70	R	MP-1	-	0.9	57	51/6	89
11	M	74	R	MP-2	-	0.6	49	35/14	71
12	M	83	R	MP-2	-	16.5	6365	5992/373	94
13*	F	50	L	MP-2	-	0.3	114	99/15	87
14*	F	63	R	MP-2	-	5.8	765	752/13	98
15	M	81	L	MP-2	BBG	7.5	1391	407/984	29
16	F	44	R	MP-2	BBG	10.4	137	109/28	80
17	M	62	R	MP-2	-	8.1	780	474/306	61
18	F	66	R	MP-2	-	23.1	7543	1876/5667	25
19*	M	45	R	MP-2	-	14	319	103/216	32
20	F	76	L	VMTS	BBG	6.2	231	150/81	65
21	F	76	L	VMTS	BBG	3.7	14	12/2	86
22	M	75	L	VMTS	BBG	1.1	126	36/90	29
23	F	62	L	VMTS	BBG	1.3	126	46/80	37
24	M	65	L	VMTS	BBG	2.8	17	3/14	18
25*	F	68	R	VMTS	-	2.7	446	389/57	87
26*	M	72	R	VMTS	-	1.8	11	5/6	45
27	F	74	R	VMTS	BBG	2.6	45	17/28	38

(*) processed 24 hours after surgical removal; (M) Male, (F) Female; (BBG) Brilliant Blue G, (-) no dye; (MP-1) MP with complete PVD, (MP-2) MP with incomplete PVD.

Figure 3.1

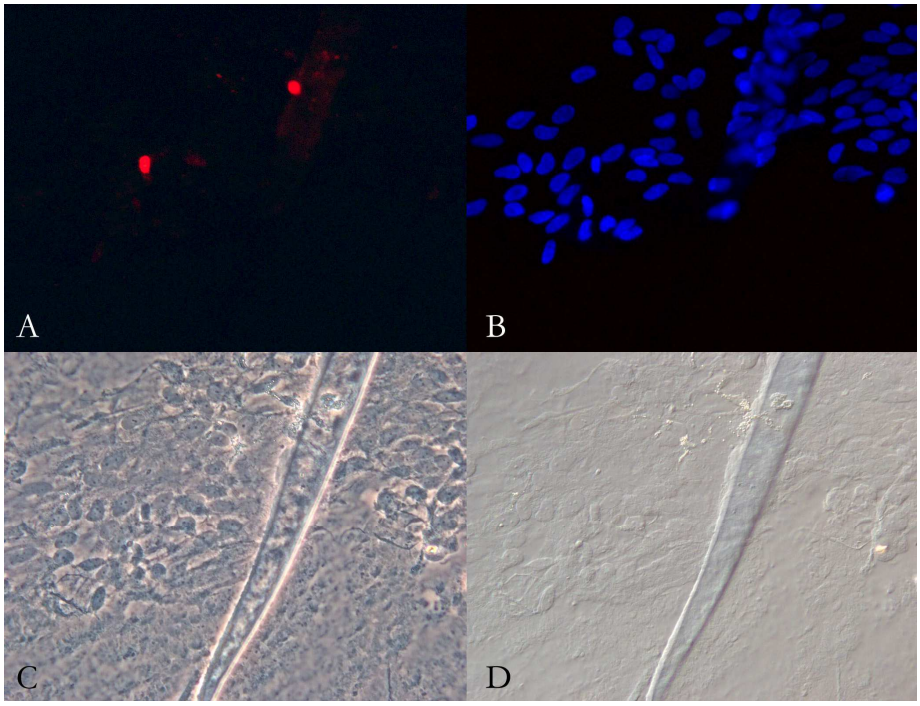

Figure 3.1 LIVE/ DEAD ® viability assay. A specimen removed from a patient with MP and incomplete PVD. (A) Dead cells bind to EthD-1 presenting as bright red cell nuclei. (B) All cells were labeled with calcerin AM presenting as blue cell nuclei. (C) Interference micrograph and (D) phase contrast micrograph of the same detail as (A) and (B) demonstrating the cells' distribution on the ILM. (Original magnification: x400)

3.2.2 Cell viability percentage and vital dye Brilliant Blue G

In this series, there were 11 specimens removed after using BBG administration into the vitreous cavity to stain the ILM during vitrectomy. In the remaining 16 cases, no dye was used to stain the ILM intraoperatively. By comparing the viability percentage of these two groups, it was found that specimens removed from eyes without BBG usage during surgery presented with significantly higher mean cell viability percentage (83%) than specimens with BBG dye (75%) ($p = 0.048$, Mann-Whitney Test). (Figure 3.2)

Figure 3.2

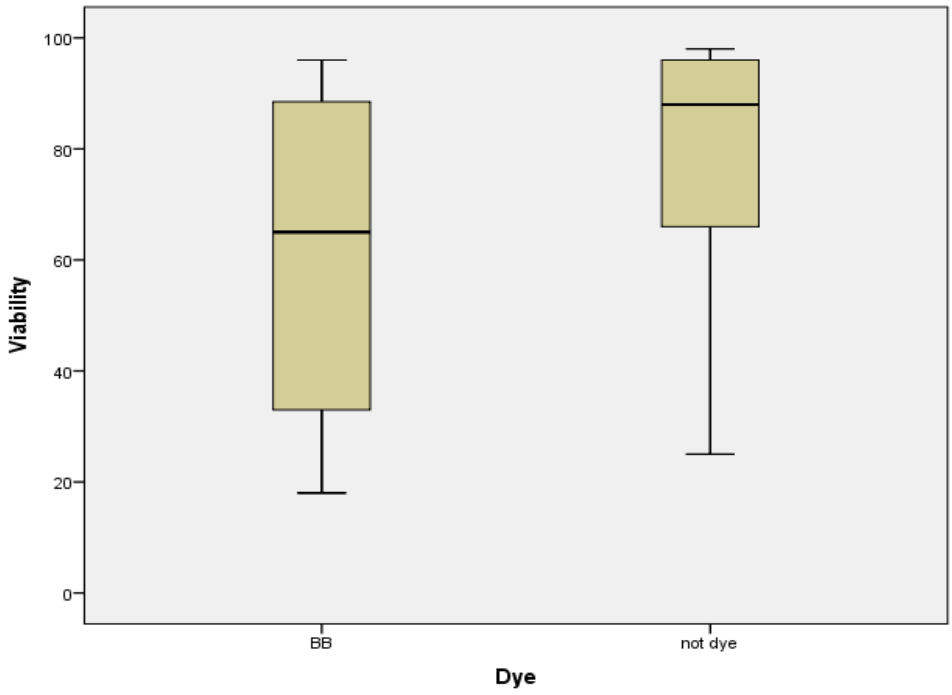

Figure 3.2 Box plot presentation shows significantly higher cell viability percentage in specimens removed without administration of BBG during surgery compared to specimens removed after administration of BBG into the vitreous cavity (p = 0.048, Mann-Whitney Test).

3.2.3 Cell viability percentage and clinical data

Specimens removed from 15 male and 12 female patients presented with average viability percentages of 86.7% and 64.6%, respectively.

Comparing the cell viability with the patients' age, the highest average viability percentage of 94% was seen in the group of 70-80 year old (n = 12). Specimens from the group of 60-70 years old patients (n = 8) were found with the lowest average cell viability percentage of 46%.

Duration of symptoms in this series ranged from 3 weeks to more than 5 years. We found that duration of symptoms less than 6 months was correlated with the highest cell viability percentage of 93%. In contrast, specimens from patients with the duration of symptoms

ranging from 6 months to 1 year presented with the lowest cell viability percentage (42%). (Table 3.2)

Table 3.2 Duration of symptoms and cell viability percentage

Duration of symptoms	Case numbers	Mean cell viability percentage (%)
< 3 months	4	93
3-6 months	6	93
6 months - 1 year	7	42
1-3 years	4	76
> 3 years	4	83
Not mentioned	2	87

3.3 Phase contrast and interference microscopy

Total cell count and cell distribution analysis included all 119 specimens. By phase contrast and interference microscopy, areas of the ILM presenting with cell proliferation were easily distinguished from areas without cell proliferation. The cell nuclei and cell extensions were clearly delineated from the ILM. Fluorescence microscopy showed the cell nuclei with blue color by DAPI stain. (Figure 3.3)

Figure 3.3

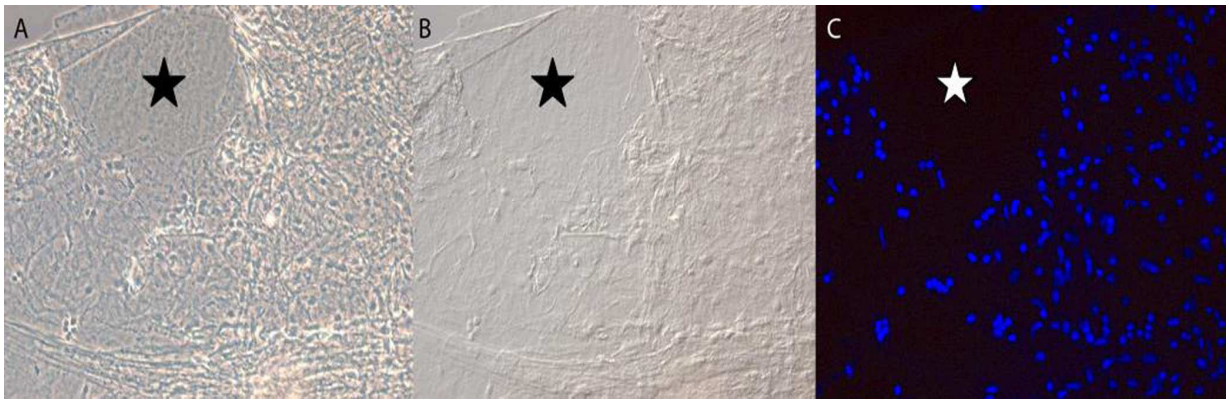

Figure 3.3 Phase contrast and interference micrographs and DAPI cell nuclei staining from a specimen removed for MP with complete PVD. (A) Phase contrast micrograph, (B) interference micrograph and (C) DAPI nuclei staining image demonstrate cell proliferation and the cells' distribution that can easily be detected and distinguished from areas with bare ILM (asterisk). (Original magnification: x200)

3.3.1 Total cell count and removed area of the ILM

All 119 specimens showed a large variety of total cell count that ranged from 0 to 20,778 with a mean of 2,550 (SD 3,930). Cell counts in specimens with homogenous cell distribution was 4,489 (SD 4,754) compared to 1,298 (SD 1,168) in specimens with cell clusters. The total area of ILM ranged from 0.3 mm^2 to 31.3 mm^2 with a mean of 8.8 mm^2 (SD 7.5 mm^2).

Specimens from eyes with MP and complete PVD seem to prevail to from eyes with MP and incomplete PVD and VMTS. However, in terms of total cell count and removed area of ILM

the difference was not statistically significant among the three groups of diagnosis (P > 0.05, Kruskal-Wallis-Test). (Table 3.3)

Table 3.3 Average areas of removed ILM and total cell counts according to the groups of diagnosis

Diagnosis	Case numbers	Average area of ILM (mm^2)	Average total cell count
MP with complete PVD	39	9.8	3,574
MP with incomplete PVD	40	9.0	2,444
VMTS	40	7.6	1,658

3.3.2 Cell distribution patterns

In almost half of all 119 cases (n = 59) examined for cell count and cell distribution analysis, cell proliferation was seen as a continuous sheet of cells homogenously distributed on the ILM (Figure 3.4). In the remaining 59 specimens, the cells were inhomogenously distributed at the ILM forming areas of cell clusters (Figure 3.5). One specimen from MP with complete PVD was found without cell proliferation but bare ILM.

Excluding the specimen removed from MP and complete PVD with bare ILM, 58.9% specimens removed from MP and complete PVD (22/38), 52.5% specimens removed from MP and incomplete PVD (21/40) and 40% specimens removed from VMTS (16/40) were distributed homogenously.

Specimens from eyes with MP showing homogenous cell distribution were seen with significantly more total cell counts (p < 0.001, Mann-Whitney Test) and larger specimen areas (p = 0.006, Mann-Whitney Test) than specimens removed from eyes with MP showing inhomogenous cell distribution with cell clusters. (Table 3.4)

Table 3.4 Cell distribution patterns with total cell counts and ILM areas

Cell distribution	Diagnosis	Cases number	Mean area of ILM (mm^2)	Mean total cell count
inhomogenous	MP with complete PVD	16	6.1	995
	MP with incomplete PVD	19	5.8	490
	VMTS	24	6.0	517
homogenous	MP with complete PVD	22	12.7	5567
	MP with incomplete PVD	21	11.9	4212
	VMTS	16	9.9	3370

Figure 3.4

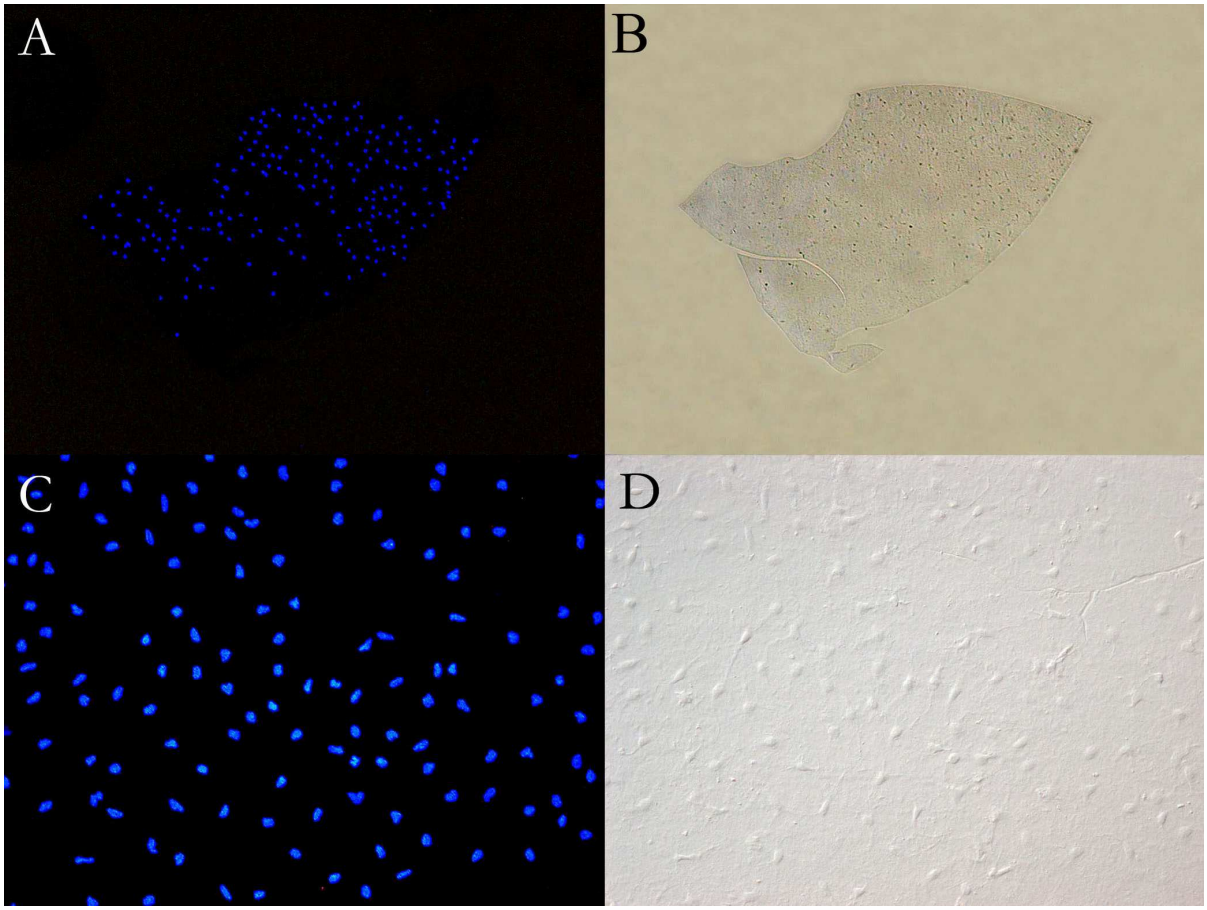

Figure 3.4 Homogenous cell distribution patterns in a specimen removed for VMTS. (A, C) DAPI cell nuclei staining fluorescence micrograph shows a continuous sheet of homogenously distributed cells on the flat-mounted ILM, (B) phase contrast micrograph and (D) interference micrograph present the same detail of the specimens. (Original magnification: A, B: x50; C, D: x200)

Figure 3.5

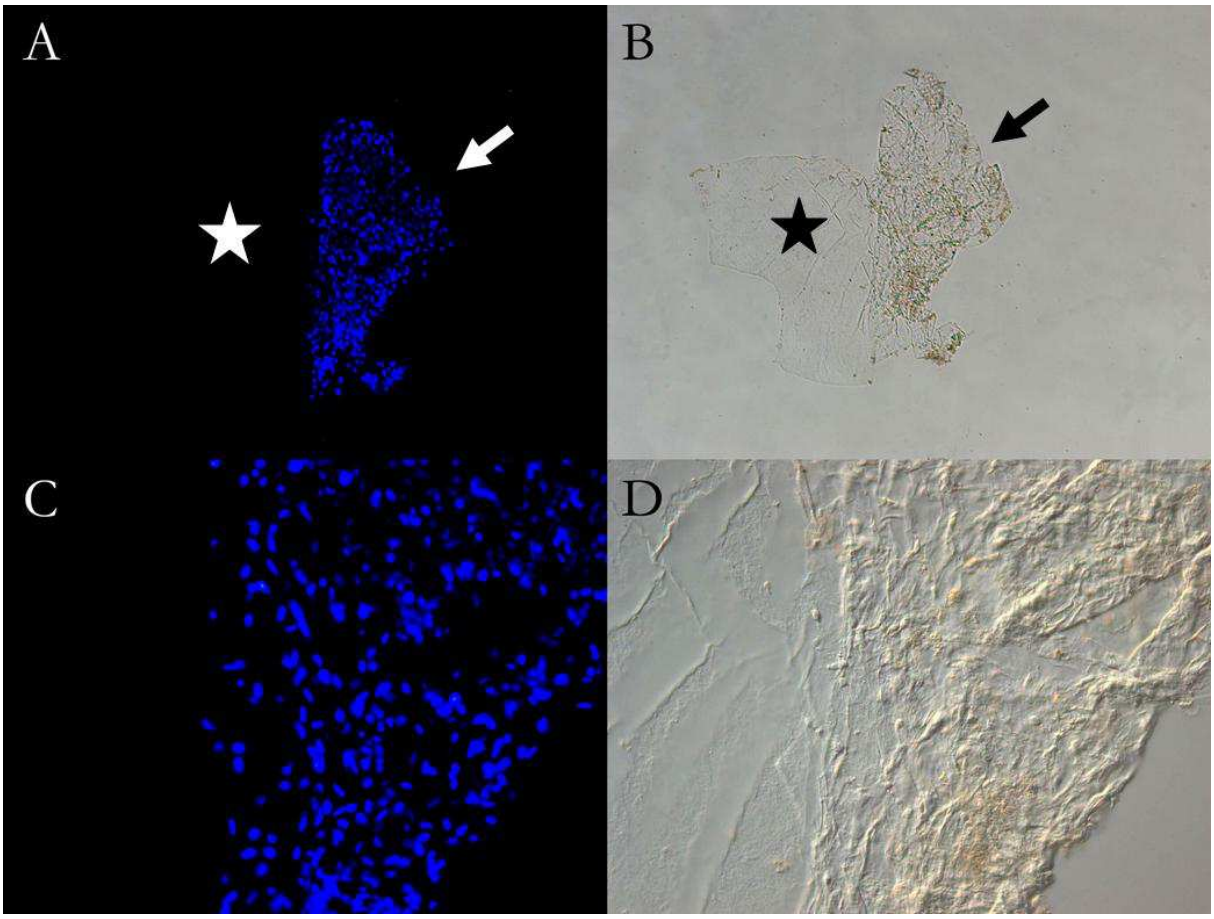

Figure 3.5 Inhomogenous cell distribution patterns with cell cluster formation in a specimen removed for MP with incomplete PVD. (A, C) DAPI cell nuclei staining fluorescence micrographs demonstrate large cell cluster with densely packed cell proliferation (arrow), (B) phase contrast micrograph and (D) interference micrograph images show corresponding details of the same specimens. Cell cluster formation (arrow) sharply delineates directly neighboring bare ILM (asterisk). (Original magnification: A, B: x50; C, D: x200)

3.4 Immunocytochemical analysis

3.4.1 General features

Twenty-seven specimens were processed by indirect immunocytochemical analysis, including 8 specimens from eyes with MP and complete PVD, 8 specimens from eyes with MP and incomplete PVD, and 11 specimens from eyes with VMTS.

Most positive immunostaining of anti-GFAP, -CD163 and –CD45, and anti-α-SMA was found in all specimens tested. Due to their predominant expression, the four antibodies were analyzed in detail in section 3.4.2.

As presented in Table 3.5 and Figure 3.6, anti-CRALBP and -vimentin were positive in all three groups of diagnosis. Anti-Kir4.1 was absent in VMTS specimens but sparsely distributed in specimens from MP. Anti-pan-cytokeratin was only present in one specimen removed from eye with VMTS; whereas, anti-GAP43 and -NF were not seen in this series. Anti-CD34 was sparsely positive in all specimens tested. Anti-CD68 was mostly demonstrated in VMTS (about 50%), but absent in specimens from MP with complete PVD. Collagen IV and fibronectin antigens were expressed in all samples. Anti-laminin was sparsely distributed in MP, irrespectively of the presence of complete or incomplete PVD. In contrast, anti-Ki67 was sparsely distributed in VMTS (less than 30%), but positive in more than 60% specimens removed from eyes with MP.

There were a proportion of cells not labeling with any cell marker combinations used in this study. These unidentified cells were negative for all cell type-specific antibodies used according to Table 3.5. Negatively labeled cells were mostly found loosely distributed as single cells at the ILM.

Table 3.5 Antibody expression according to diagnosis

Anti-	Positive labeled cells expressed in		
	MP with complete PVD (n = 8)	MP with incomplete PVD (n = 8)	VMTS (n = 11)
CD163	+	+	+
CD45	+	+	+
GFAP	+	+	+
Vimentin	**(+)**	+	+
CRALBP	+	+	+
Kir4.1	**(+)**	**(+)**	-
α-SMA	+	+	+
pan-Cytokeratin	-	-	**(+)**
GAP43	-	-	-
NF	-	-	-
CD34	**(+)**	**(+)**	**(+)**
CD68	-	**(+)**	+
Collagen IV	+	+	+
Fibronectin	+	+	+
Laminin	**(+)**	**(+)**	+
Ki67	+	+	**(+)**

- absent; (+) sparse; + present

Figure 3.6

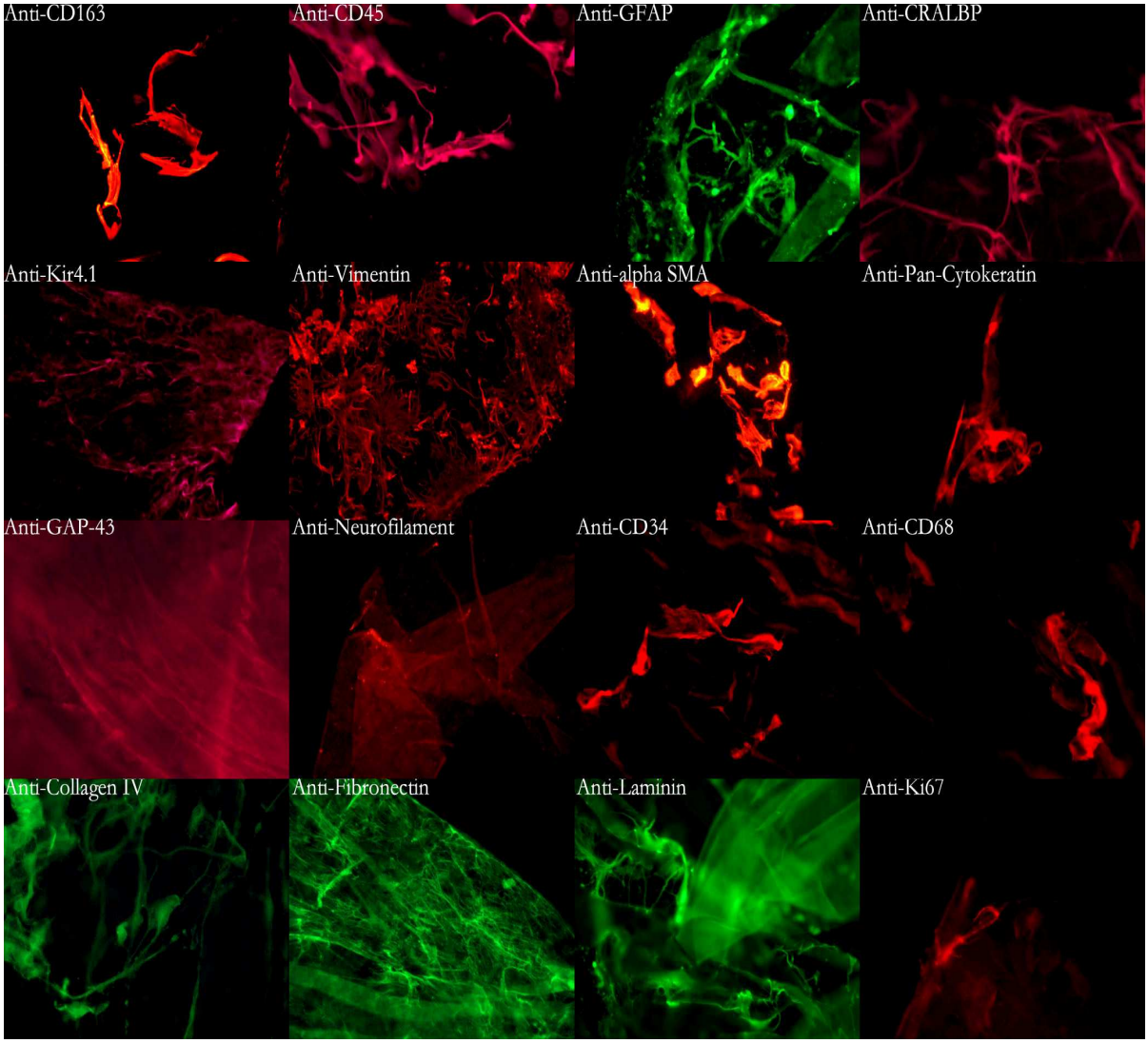

Figure 3.6 Immunoreactivity of all 16 antibodies used in this study. Except for negative signals in anti-GAP43 and anti-neurofilament labeling, all antibodies demonstrated positive immunoreactivity that was at least sparsely distributed on flat-mounted ILM specimens. (Original magnification: Anti-CD163 x200, Anti-CD45 x400, Anti-GFAP x400, Anti-CRALBP x400, Anti-Kir4.1 x200, Anti-vimentin x100, Anti-alpha SMA x200, Anti-pan-cytokeratin x200, Anti-GAP43 x400, Anti-neurofilament x200, Anti-CD34 x400, Anti-CD68 x400, Anti-collagen IV x400, Anti-fibronectin x400, Anti-laminin x400, Anti-Ki67 x400)

3.4.2 Antigen expression of CD163, CD45, GFAP and α-SMA

Immunocytochemical analysis of anti-CD163, -CD45, -GFAP, - and -α-SMA labeling was performed in the 24 specimens. According to Table 3.6, we found that (1) anti-CD163 labeling presented predominantly in MP with complete PVD compared to other groups of diagnosis; (2) α-SMA labeling mainly presented in MP with incomplete PVD and VMTS; (3) anti-GFAP labeling was found in both MP groups, irrespectively of the extent of PVD; and (4) anti-CD45 expressions were similar in all three groups of diagnosis.

Table 3.6 Detailed antibody analysis according to diagnosis

Anti-	Antibody-labeled cells expression in		
	MP with complete PVD (n=8)	MP with incomplete PVD (n=8)	VMTS (n=8)
CD163	++	+	+
CD45	+	+	+
GFAP	++	++	+
α-SMA	+	++	++

- absent; (+) sparse; + some; ++ many

3.4.3 Simultaneous cell-type specific antigen expression

Most importantly, there were co-localizations of cell type specific antibodies seen, including anti-GFAP/CD45, anti-GFAP/CD163, anti-CD163/CD45, and anti-CD163/α-SMA (Figure 3.7).

When labeled with anti-GFAP, anti-CD45 was concomitantly co-localized with anti-GFAP. We found co-localization of these two antibodies in almost 20% specimens tested. Co-localizations of anti-CD163/GFAP and anti-CD163/CD45 were sparsely present. (Figure3.8)

Co-localization of anti-CD163 and anti-α-SMA was only seen in single cases. There was no apparent co-expression of α-SMA and GFAP or α-SMA and CD45 in any specimens examined. Other cell markers such as anti-CRALBP and –vimentin were simultaneously expressed in 67% of tested specimens. However, there was no evidence of co-localization of anti-CRALBP or –vimentin with anti-GFAP.

Figure 3.7

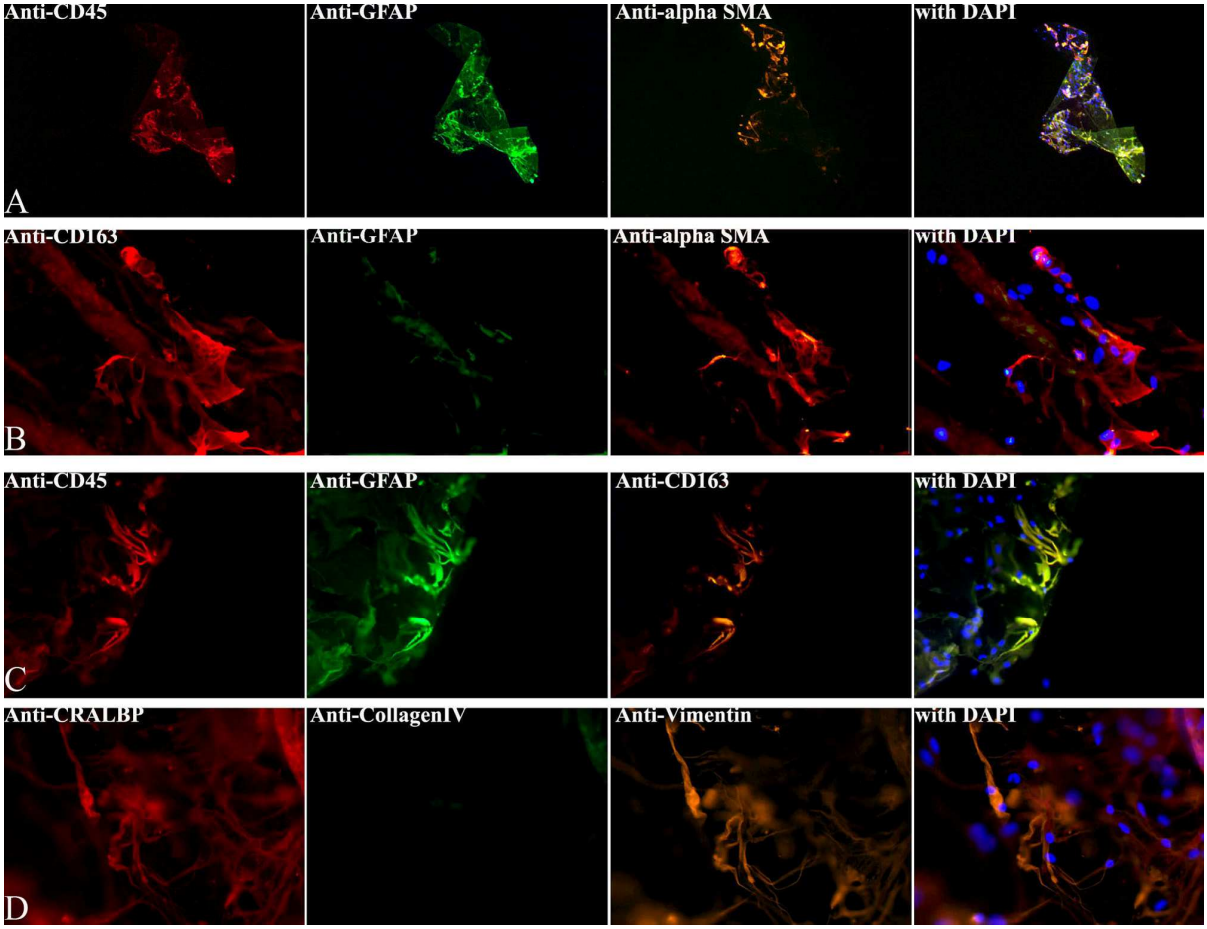

Figure 3.7 Fluorescence micrographs demonstrating antibody co-localizations according to their antibody combinations tested and in combination with a merged figure with DAPI cell nuclei staining. (A) Co-localization of anti-GFAP/CD45 with different labeling patterns of anti-α-SMA. (B) Co-localization of anti-CD163/α-SMA with negative labeling of anti-GFAP. (C) Co-localization of anti-GFAP/CD163 and anti-GFAP/CD45. (D) Co-localization of anti-CRALBP/vimentin. (Original magnification: (A) x50; (B) x400; (C) x200; (D) x400)

Figure 3.8

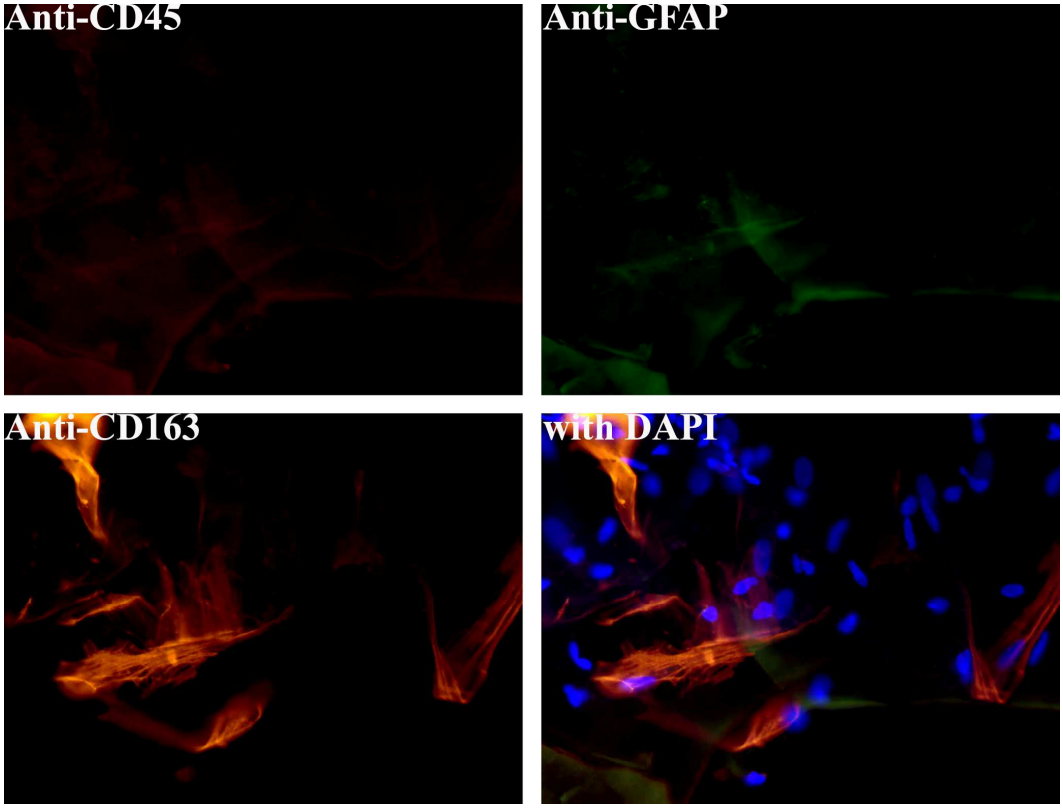

Figure 3.8 Fluorescence micrographs of anti-CD163, -CD45 and –GFAP labeling. In contrast to other specimens, this specimen shows positive immunoreactivity for anti-CD163, whereas anti-CD45 and -GFAP were negative. (Original magnification: x400)

3.4.4 Negative control

Whenever more than two parts of specimens from one patient were obtained, we were able to perform indirect immunofluorescence evaluation with more than one combination of three antibodies. In all control specimens, when the primary antibody was substituted by diluent, no immunoreactivity was observed. (Figure 3.9)

Figure 3.9

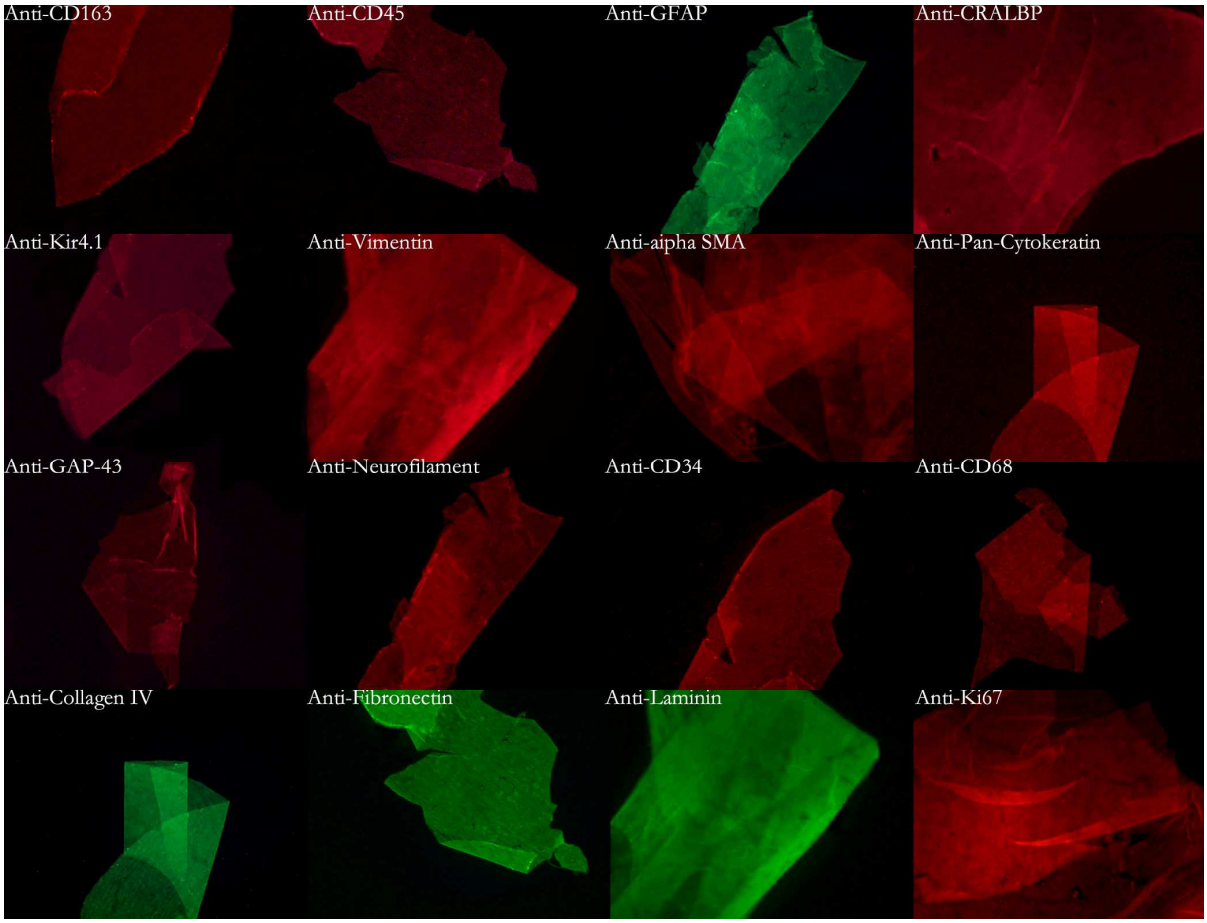

Figure 3.9 Fluorescence micrographs of negative controls of immunocytochemical labeling. (Original magnification: Anti-CD163 x50, Anti-CD45 x50, Anti-GFAP x100, Anti-CRALBP x400, Anti-Kir4.1 x50, Anti-vimentin x200, Anti-alpha SMA x400, Anti-pan-cytokeratin x50, Anti-GAP43 x50, Anti-neurofilament x100, Anti-CD34 x50, Anti-CD68 x50, Anti-collagen IV x200, Anti-fibronectin x50, Anti-laminin x50, Anti-Ki67 x200)

4. Discussion

4.1 Flat-mount preparation

Since ILM peeling with ERM removal became a routine approach to relieve vitreomacular traction during vitreoretinal surgery, harvested ILM specimens were conventionally processed for embedding and sectioning preparation procedures in the past. Recently, a new preparation technique was proposed, the flat-mounted specimen preparation method, and a relatively few numbers of ILM specimens were studied using this method to date. [Hisatomi, 2005; Hisatomi, 2006; Gandorfer, 2009]

The flat-mount preparation method has numerous advantages compared to conventional cross-sectioning preparation procedures. Most importantly, by mounting whole ILM specimens on a glass slide the new method enables to show the maximum area of a tissue specimen with en-face observation of the total cell distribution. Not a single cell is missed to be analyzed. In contrast, by conventional serial sectioning of ILM specimens a relatively small part of the ILM specimen is seen. Gandorfer and colleagues assumed that no more than 6% of the total peeled ILM area would be investigated under the microscope by serial sectioning preparation of ILM specimens. [Gandorfer, 2009] Thus, only a minor part of the specimen is analyzed possibly missing important details. Using the flat-mount preparation procedure in a large number of specimens, stage II macular holes were reported for the first time to present cell proliferation on the ILM in all cases. [Schumann, 2011] Most probably, epiretinal cell proliferation was missed in earlier studies using embedding and cross-section techniques. Using the new preparation method, surgical specimens were screened for pores in the ILM since cross-section preparation of ILM specimens does not allow for determining the incidence of ILM pores regarding the small area of interest. [Gandorfer, 2011] Thereby, it became possible to demonstrate that ILM pores are rather a rare finding and that they are less frequently found than formerly presumed.

Furthermore, cell proliferation in flat-mounted ILM specimens can be easily examined by different techniques without changing the protocol. Interference microscopy and phase contrast microscopy are performed without additional tissue staining. Time consuming embedding procedures are not needed. Immunocytochemical staining techniques can be processed on flat-mounted specimen, thus allowing for direct correlation of microscopic

findings with cell-specific immunoreactivity. Cell nuclei staining and live-dead cell viability testing are possible to obtain accurate results analyzing cell distribution and the cells' viability. Of note, after analysis, flat-mounted ILM specimens can still be processed for further embedding and cross-sectioning procedures, such as transmission electron microscopy, according to conventional protocols.

However, the new flat-mounted specimen preparation procedure does have some limitations with regard to morphological topography and variety of immunocytochemical antibody combinations. By microscopic analysis of flat-mounted ILM specimens, it is not yet possible to determine if cellular elements are adjacent to the vitreal or to the retinal side of the ILM. The amount and the type of collagen at the ILM and within cell proliferations can not be specified by interference or phase contrast microscope alone. Immunocytochemical analysis helps to identify the type of collagen although with our laboratory setting no more than three antibody combinations could be tested at once.

4.2 Cell viability

This is the first study performing cell viability investigation of ILM specimens. Whereas in embedding and sectioning techniques numerous fixatives and solutions become necessary to process the surgically removed tissue, in flat-mount preparation native tissue can be examined. This allows for new applications and purposes in studying cell proliferation of ILM specimens.

Comparing specimens removed from eyes with MP or VMTS, we found significant differences in cell viability. Specimens removed from eyes with MP (76.9%) presented with higher cell viability than specimens removed from eyes with VMTS (64.8%). In detail, specimens from MP with complete PVD (94.5%) were found with significantly higher cell viability than specimens from MP with incomplete PVD (56.4%). These findings raise the hypothesis that the extent of PVD or vitreoretinal adhesion with traction forces may have some influence on cell viability of epiretinal cells, although a causative correlation can not be determined by this study. Cell viability measurements assess healthy cells in tissue independent if these cells are actively dividing or if they are quiescent. Of note, cell viability analysis provides no information on proliferation potential. The fact that epiretinal membranes from eyes with complete PVD show significantly more viable cells than eyes with persistent vitreoretinal adhesion or even antero-posterior vitreoretinal traction may be due to a higher cell turnover in the latter ones. One might hypothesize that severe vitreoretinal traction modulates tissue homeostasis in epiretinal membranes which is a dynamic balance between cell growth, cell proliferation and cell death in order to regulate morphology and function. [Meth, 2000] However, further investigations with measurement of cell proliferation and apoptosis are needed to elucidate that question.

One might argue that differences in cell viability percentages of specimens removed from MP or VMTS may be due to discontinuity of specimen preparation, although we defined tissue processing immediately after surgical removal precisely using the same procedure. To improve our understanding of cell death and cell viability after ILM/ ERM peeling, we examined six specimens with a time delay of 24 hours after their removal with meanwhile storage in BSS at +4°C. These specimens were expected to present lower cell viability percentages than specimens immediately processed after surgery. Interestingly, these six specimens (one specimen from MP with complete PVD, three specimens from MP with

incomplete PVD, and two specimens from VMTS) were found with a mean viability percentage of 83% (SD 28%) that ranged from 32% to 98%. Since time delay in specimens' preparation did not significantly lowered cell viability, we assume that difference in specimens removed from MP and VMTS as reported above are rather related to disease characteristics than to tissue processing.

Furthermore, our results demonstrate that epiretinal tissue removed after intraoperative administration of BBG (75%) presents significantly lower cell viability that epiretinal membranes removed without using BBG (83%) as vital dye during vitreoretinal surgery. Brilliant blue G was always considered to be a safe vital dye without retinal toxicity when applied in low dose for a short period of time in routine settings. [Schumann, 2009; Schumann, 2010; Morales, 2010; Haritoglou, 2011; Hönig, 2011] In clinical studies, there was no retinal toxicity or adverse effects related to the BBG reported. Therefore, BBG became generally accepted in routine macular surgery for specific ILM staining. However, this is the first study comparing cell viability of removed ILM/ERM specimens with and without administration of BBG during vitrectomy. Based on our results, it appears that BBG may have some effect on epiretinal cells even in routine surgical setting.

4.3 Cell distribution patterns

In accordance to previous studies, we found massive cell proliferation in ILM specimens removed during macular surgery for MP and VMTS. [Heidenkummer, 1992; Gastaud, 2000; Gandorfer, 2005; Sebag, 2007; Schumann, 2010] However, cell count and cell distribution of ILM/ERM specimens have not been analyzed before by flat-mount preparation although morphological studies precisely described cell proliferations in MP and VMTS by sectional preparation in the past.

Herein, we report that specimens removed from eyes with MP, irrespective of the presence of PVD, presented with significantly higher total cell counts than specimens removed from eyes with VMTS. However, given the fact that we found a large variety of removed specimen areas in both diseases, total cell numbers remain difficult to interpret. Importantly, we found two cell distribution patterns in specimens removed from MP and VMTS, the homogenous cell distribution and the cell cluster formation. Both distribution patterns were reported in flat-mounted ILM specimens removed from eyes with idiopathic macular holes as well. [Schumann, 2011] In this study, specimens from MP demonstrated both distribution patterns that showed no difference comparing specimens removed from eyes with complete or incomplete PVD. In specimens from VMTS, cell cluster formation was more frequently (24/40 specimens) found than homogenous cell distribution. One might speculate if epiretinal cell proliferation may be initiated by localized vitreoretinal traction forming cell clusters that progress to homogenous cell multilayers at the vitreal side of the ILM. In that context, retinal Müller glial cells are thought to become activated by vitreoretinal traction. It is hypothesized that activated RMCs migrate through the ILM on its vitreal surface where they are believed to form epiretinal cell proliferations. [Bringmann and Wiedemann, 2009]

4.4 Antigen expression

4.4.1 General expression

In order to determine the pathologic relation between the vitreous, the retina and epiretinal tissue, numerous studies described morphological features of ERMs in detail. [Hiscott, 1983; Smiddy, 1989; Heidenkummer, 1996; Schumann, 2010] Immunohistochemical examinations were performed by cross-sectional preparation techniques to add information on cell types and the cells' origin involved in ERM formation in MP and VMTS. [Hiscott, 1984; Heidenkummer, 1992; Shinoda, 2000] However, this is the first study reporting on antigen expression in a large series of flat-mounted ILM/ERM specimens removed from MP and VMTS. Herein, we present evidence that glial cells and hyalocytes seem to be predominant in epimacular tissue from MP and VMTS.

Glial cell marker such as GFAP, vimentin and CRALBP were demonstrated in specimens from MP and VMTS, irrespective of the presence of PVD. Glial fibrillary acidic protein constitutes of glial intermediate filaments in astrocytes of the retina. It is not or very faintly expressed in RMCs, except at their endfeet. However, in pathologic conditions RMCs become activated. Thereby, they were shown to up-regulate GFAP in response to injury or stress, such as tractional forces mediated from the vitreous to the retina. [Uhlmann, 2003; Bringmann, 2006] Retinal Müller glial cells, normal and reactive astrocytes are also known to be positive for vimentin. [Nakazawa, 2007; Luna, 2010] Kir4.1 is found on RMC endfeet membranes. [Higashimori, 2007; Ruiz-Ederra, 2007] Furthermore, RMCs as well as RPE cells were demonstrated to be immunoreactive for CRALBP. [Collery, 2008; Huang, 2009] In this study, immunostaining for pan-cytokeratin was negative in MP and sparsely positive in VMTS. Kir4.1 was found positive in MP. Vimentin and CRALBP were seen in MP and VMTS in similar distribution. Thus, we postulate that rather glial cells than RPE cells predominated in our specimens. This is in contrast to previous studies reporting on the presence of RPE cells in idiopathic MP, and demonstrating the absence of RPE cells in VMTS. [Smiddy, 1989; Shinoda, 2000] Based on our results, we support the hypothesis that glial cells, notably RMCs, are an important component of epiretinal membranes in both MP and VMTS which is in accordance to previous ultrastructural and immunohistochemical findings. [Hiscott, 1983; Shinoda, 2000; Gastaud, 2000; Snead, 2004]

Hyalocyte marker such as CD45 and CD163 were similarly demonstrated in specimens from MP and VMTS in this study. Hyalocytes are known to be immunoreactive for CD45, CD64 and CD163, to belong to the monocyte/macrophage lineage, and to derive from bone marrow. [Lazarus, 1994; Zhu, 1999; Sakamoto, 2003; Qiao. 2005; Sakamoto, 2011] According to their morphology, hyalocytes are described as resembling macrophages. However, a variety of morphological features of hyalocytes can be found in cells of the same population. It is questionable, if this heterogeneity is related to different origins of cells or to different states of cell metabolism and activity. Being rather a heterogeneous population of cells, hyalocytes were reported to be replaced in the vitreous within seven months under physiological conditions. [Qiao, 2005]

Myofibroblast-like cells, being immunoreactive for α-SMA, represent contractile properties of epiretinal tissue possibly as a consequence of cell transdifferentiation. In this study, they were more frequently found in specimens from VMTS and MP with incomplete PVD than in specimens from MP with complete PVD. Myofibroblast-like cells are of unknown origin possessing contractile elements. They are typically found in ERMs from VMTS as reported in the past. [Shinoda, 2000; Gandorfer, 2002; Gandorfer, 2005] However, myofibroblasts are not restricted to membranes derived from VMTS, but rather can be found in all epiretinal tissue that exerts traction at the retina such as ERMs in macular holes, diabetes retinopathy, and idiopathic MP. [Smiddy, 1992; Abu El-Asrar, 2006; Schumann, 2006; Schumann, 2008]

The cell surface marker CD68 characterizes macrophages and microglia. [Elner, 1992; Streit, 2001; Zeng, 2008; Akrami, 2011] In this study, CD68 was demonstrated in VMTS and MP with incomplete PVD. CD68 was not found in specimens from MP with complete PVD. There is no cell-specific marker to differentiate between vitreous derived macrophages and retinal microglia. With regard to our results, it appears that vitreoretinal traction might be related to the presence of macrophages or microglia in ERMs.

CD34 is known to be expressed in endothelial cells of retinal and choroidal blood vessels. [Barcelona, 2010] Since anti-CD34 was sparsely positive in all specimens tested in this study, we speculate that endothelial cells or endothelial precursor cells do not compose a major component of epiretinal tissue in MP and VMTS.

Collagen IV, fibronectin and laminin was found in all specimens removed from eyes with MP and VMTS that were examined in this study, which is in accordance with numerous previous reports. [Lesnik Oberstein, 2008; Ponsioen, 2008; Chen, 2009; Li, 2009]

The proliferation marker Ki67 was positive in more than 60% of all tested specimens from eyes with MP in this study, but it was sparsely expressed in VMTS (below 30%). However, we found no evidence to specify the exact cell types which was related to the limitation of three antibody combinations.

Anti-GAP43 and -NF were not seen in this series which is in contrast to previous examinations. [Sethi, 2005; Ivanov, 2006; Chen, 2008; Gandorfer, 2009; Lesnik Oberstein, 2011] Anti-NF labelled processes were demonstrated in idiopathic epiretinal membranes representing neurites that were presumed to originate from retinal ganglion cells. [Lesnik-Oberstein, 2008] GAP-43 expression was reported to be up-regulated in retinal ganglion cells and reactive RMCs upon retinal injury indicating that there is remodelling with some neuronal plasticity after retinal damage. [Dijk, 2007] However, the findings of this study do not support this hypothesis.

Since a proportion of cells were not labeled with any cell marker combination used in this study, we presume there are either (1) cells that are non-viable, or (2) dedifferentiated progenitor cells, or (3) transdifferentiated cells that were not detected by the commonly used immunocytochemical antibodies. Cell transdifferentiation still complicates the determination of the cells' phenotype and origin, because there is no specific marker of it.

4.4.2 Simultaneous antigen expression

Co-localizations of the glial cell marker anti-GFAP and the hyalocyte markers anti-CD45 and anti-CD163 as demonstrated in this study have not been described before in human ILM-specimens removed for MP and VMTS. Furthermore, we found co-localization of anti-α-SMA with the hyalocyte marker anti-CD163. Other co-localizations that were observed in this study such as anti-CD163/CD45 and anti-CRALBP/vimentin have not been demonstrated in flat-mounted ILM specimens so far, but they are an expected finding according to previous reports on hyalocyte and glial cell antigen expressions. [Guérin, 1990; Lazarus, 1994; Sakamoto, 2003; Sakamoto, 2011]

Co-localization of hyalocyte and glial cell markers was recently described in ILM specimens removed from idiopathic macular holes. [Schumann, 2011] It appears that GFAP labeling in epiretinal cell proliferation needs to be reconsidered since positive GFAP labeling no longer allows for determination of cells to be of glial origin. There are two hypotheses that may arise considering our findings. First, cells with double labeling for anti-GFAP and hyalocyte markers may represent hyalocytes. Hyalocytes with positive GFAP expression have already been described in other species. GFAP-positive hyalocytes were reported in porcine, pecteneal, and bovine hyalocyte cell lines. [Nishitsuka, 2007; Llombart, 2009; Kohno, 2009] However, it is unknown if these 'hyalocytes' expressed GFAP endogenously or if they contained GFAP from other origin due to their well-known phagocytic activity. Another hypothesis is that double labeled cells may represent progenitor cells.

Co-localization of anti-CD163/α-SMA indicates that hyalocytes may transdifferentiate into myofibroblast-like cells. Myofibroblast-like transdifferentiation with positive α-SMA expression has been shown for both glial cells and hyalocytes. [Hirayama, 2004; Kohno, 2009; Sakamoto, 2011] Thus, our results support the hypothesis that hyalocytes are able to transdifferentiate into myofibroblast-like cells in epiretinal membranes.

4.4.3 Contractility and posterior vitreous detachment

Wrinkling of the ILM with underlying retinal layers is a consistent feature in traction maculopathies such as MP and VMTS. Epiretinal cell proliferation with contractile properties is generally accepted as a morphological correlate in the formation of tangential traction at the retina. [Morris, 2000] Most important, contractile elements in epiretinal tissue are presumed to be myofibroblasts. [Hiscott, 1983; Shinoda, 2000]

As mentioned above, positive α-SMA labeled epiretinal cells mainly presented in MP with incomplete PVD and VMTS compared to MP with complete PVD. Thus, we hypothesize that the extent of PVD with persistent vitreoretinal adhesions may play an important role in the differentiation of epiretinal cells and their antigen expression in eyes with MP and VMTS. Persistent vitreoretinal adhesions due to incomplete PVD cause antero-posterior vitreoretinal traction at the ILM and retinal layers. [Koerner, 1999; Gandorfer, 2005; Sebag, 2008] It has previously been proposed that retinal Müller cells become activated by antero-posterior vitreoretinal traction in the context of incomplete PVD. [Bringmann, 2006] They are thought to migrate from the retinal onto the vitreal side of the ILM, where they consequently

proliferate and form epiretinal membranes. However, hyalocytes were not yet reported to become influenced by vitreoretinal traction, thereby changing their phenotype with α-SMA expression. Since this study presents microscopic observations but no causative correlations, further investigation is needed to elucidate the influence of persistent vitreoretinal adhesions on the behavior of epiretinal cells.

4.5 Future prospects

Previous studies have shown that Müller glial cells express the neuronal progenitor cell marker nestin in human retina. [Luna, 2010] Microglia and macroglia were reported to derive from one progenitor cell, and to derive from bone marrow mesenchymal stem cells expressing variable amounts of GFAP. [Fedoroff, 1997; Zhang, 2004] For a more detailed understanding of transdifferentiation and the cells' origin, further investigations of epiretinal cell proliferation will be needed. Detection of neuronal progenitor cells in epiretinal membranes may be of importance and should be addressed in the future.

5. References

Abu El-Asrar AM, Struyf S, Kangave D, et al. Chemokines in proliferative diabetic retinopathy and proliferative vitreoretinopathy. *Eur Cytokine Netw*. 2006; 17(3):155-165.

Akrami H, Soheili ZS, Sadeghizadeh M, et al. Evaluation of RPE65, CRALBP, VEGF, CD68, and tyrosinase gene expression in human retinal pigment epithelial cells cultured on amniotic membrane. *Biochem Genet*. 2011; 49(5-6):313-322.

Ammar DA, Noecker RJ, Kahook MY. Effects of benzalkonium chloride-preserved, polyquad-preserved, and sofZia-preserved topical glaucoma medications on human ocular epithelial cells. *Adv Ther*. 2010; 27(11): 837-845.

Balazs EA, Toth LZ, Eckl EA, Mitchell AP. Studies on the structure of the vitreous body. XII. Cytologicall and histochemical studies on the cortical tissue layer. *Exp Eye Res*. 1964; 3:57-71.

Barcelona PF, Luna JD, Chiabrando GA, et al. Immunohistochemical localization of low density lipoprotein receptor-related protein 1 and alpha(2)-Macroglobulin in retinal and choroidal tissue of proliferative retinopathies. *Exp Eye Res*. 2010; 91(2):264-272.

Berninger B. Making neurons from mature glia: a far-fetched dream? *Neuropharmacology*. 2010; 58(6):894-902.

Bhatia B, Singhal S, Lawrence JM, et al. Distribution of Müller stem cells within the neural retina: evidence for the existence of a ciliary margin-like zone in the adult human eye. *Exp Eye Res*. 2009; 89(3):373-382.

Bongcam-Rudloff E, Nistér M, Betsholtz C, et al. Human glial fibrillary acidic protein: complementary DNA cloning, chromosome localization, and messenger RNA expression in human glioma cell lines of various phenotypes. *Cancer Res.* 1991; 51(5):1553–1560.

Bosman C, Camassei FD, Boldrini R, Corsi A. Evidence for a hybrid macrophage phenotype in erythrophagocytic histiocytosis. *J Pediatr Hematol Oncol*. 1999; 21(1):31-37.

Boyd ZS, Raja R, Johnson S, et al. A tumor sorting protocol that enables enrichment of pancreatic adenocarcinoma cells and facilitation of genetic analyses. *J Mol Diagn*. 2009; 11(4):290-297.

Bringmann A, Pannicke T, Grosche J, et al. Mülller cells in the healthy and diseased retina. *Prog Retin Eye Res*. 2006; 25(4):397-424.

Bringmann A, Pannicke T, Biedermann B, et al. Role of retinal glial cells in neurotransmitter uptake and metabolism. *Neurochem Int*. 2009; 54(3-4):143-160.

Bringmann A, Wiedemann P. Involvement of Müller glial cells in epiretinal membrane formation. *Graefes Arch Clin Exp Ophthalmol*. 2009; 247(7):865-883.

Chen M, Muckersie E, Robertson M, et al. Characterization of a spontaneous mouse retinal pigment epithelial cell line B6-RPE07. *Invest Ophthalmol Vis Sci.* 2008; 49(8):3699-3706.

Chen W, Mo W, Sun K, et al. Microplasmin degrades fibronectin and laminin at vitreoretinal interface and outer retina during enzymatic vitrectomy. *Curr Eye Res*. 2009; 34(12):1057-1064.

Collery R, McLoughlin S, Vendrell V, et al. Duplication and divergence of zebrafish CRALBP genes uncovers novel role for RPE- and Muller-CRALBP in cone vision. *Invest Ophthalmol Vis Sci.* 2008; 49(9):3812-3820.

Connors NC, Kofuji P. Potassium channel Kir4.1 macromolecular complex in retinal glial cells. *Glia*. 2006; 53(2): 124-131.

Cox MS, Azen SP, Barr CC, et al. Macular pucker after successful surgery for proliferative vitreoretinopathy. Silicone Study Report 8. *Ophthalmology*. 1995; 102(12):1884-1891.

Dellaporta A. Macular pucker and peripheral retinal lesions. *Trans Am Ophthalmol Soc.* 1973; 71:329-338; discussion 338-340.

Dijk F, Bergen AA, Kamphuis W. GAP-43 expression is upregulated in retinal ganglion cells after ischemia/reperfusion-induced damage. *Exp Eye Res*. 2007; 84(5):858-867.

Duncan DD, Fischer DG, Dayton A, Prahl SA. Quantitative Carré differential interference contrast microscopy to assess phase and amplitude. *J Opt Soc Am A Opt Image Sci Vis*. 2011; 28(6):1297-1306.

Dupont KM, Sharma K, Stevens HY, et al. Human stem cell delivery for treatment of large segmental bone defects. *Proc Natl Acad Sci U S A*. 2010; 107(8):3305-3310.

Eberhardt C, Amann B, Stangassinger M, et al. Isolation, characterization and establishment of an equine retinal glial cell line: a prerequisite to investigate the physiological function of Müller cells in the retina. *J Anim Physiol Anim Nutr (Berl)*. 2011; Apr 30. doi: 10.1111/j. 1439-0396. 2011.01447.x.

Elner SG, Elner VM, Nielsen JC, et al. CD68 antigen expression by human retinal pigment epithelial cells. *Exp Eye Res*. 1992; 55(1):21-28.

Enaida H, Hisatomi T, Hata Y, et al. Brilliant blue G selectively stains the internal limiting membrane/brilliant blue G-assisted membrane peeling. *Retina*. 2006; 26(6):631-636.

Eyden B. The fibronexus in reactive and tumoral myofibroblasts: further characterisation by electron microscopy. *Histol Histopathol*. 2001; 16(1):57-70.

Eyden B, Banerjee SS, Shenjere P, Fisher C. The myofibroblast and its tumors. *J Clin Pathol*. 2009; 62(3):236-249.

Fedoroff S, Zhai R, Novak JP. Microglia and astroglia have a common progenitor cell. *J Neurosci Res*. 1997; 50(3):477-486.

Figus M, Carpineto P, Romagnoli M, et al. Optical coherence tomography findings of incomplete posterior vitreoschisis with vitreomacular traction syndrome and impending macular hole: a case report. *Eur J Ophthalmol*. 2008; 18(1):147-149.

Fisher SK, Lewis GP, Linberg KA, et al. Cellular remodeling in mammalian retina induced by retinal detachment. In: Kolb H, Fernandez E, Nelson R, editors. Webvision: The Organization of the retina and visual system [Internet]. Salt Lake City (UT): University of Utah Health Sciences Center; 1995-. 2005 May 01 [updated 2007 Jul 03].

Franke WW, Schmid E, Osborn M, Weber K. Intermediate-sized filaments of human endothelial cells. *J Cell Biol*. 1979; 81(3):570–580.

Foos RY. Vitreoretinal juncture; topographical variations. *Invest Ophthalmol.* 1972; 11(10):801-808.

Foos RY. Nonvascular proliferative extraretinal retinopathies. *Am J Ophthalmol*. 1978; 86(5):723-725.

Fuchs U, Kivelä T, Tarkkanen A. Cytoskeleton in normal and reactive human retinal pigment epithelial cells. *Invest Ophthalmol Vis Sci*. 1991; 32(13):3178-3186.

Fuchs E, Weber K. Intermediate filaments: structure, dynamics, function, and disease. *Annu Rev Biochem.* 1994; 63:345–382.

Gandorfer A, Rohleder M, Kampik A. Epiretinal pathology of vitreomacular traction syndrome. *Br J Ophthalmol*. 2002; 86(8):902-909.

Gandorfer A, Haritoglou C, Kampik A, Charteris D. Ultrastructure of the vitreoretinal interface following removal of the internal limiting membrane using indocyanine green. *Curr Eye Res*. 2004; 29(4-5):319-320.

Gandorfer A, Rohleder M, Charteris D, et al. Ultrastructure of vitreomacular traction syndrome associated with persistent hyaloid artery. *Eye (Lond)*. 2005; 19(3):333-336.

Gandorfer A, Scheler R, Schumann R, et al. Interference microscopy delineates cellular proliferation on flat mounted internal limiting membrane specimens. *Br J Ophthalmol*. 2009; 93(1):120-122.

Gandorfer A, Schumann RG, Scheler R, et al. Pores of the inner limiting membrane in flat-mounted surgical specimens. *Retina*. 2011; 31(5):977-981.

Gastaud P, Bétis F, Rouhette H, Hofman P. Ultrastructural findings of epimacular membrane and detached posterior hyaloid in vitreomacular traction syndrome. *J Fr Ophthalmol*. 2000; 23(6):587-593.

Gering E, Atkinson CT. A rapid method for counting nucleated erythrocytes on stained blood smears by digital image analysis. *J Parasitol*. 2004; 90(4):879-881.

Guérin CJ, Anderson DH, Fisher SK. Changes in intermediate filament immunolabeling occur in response to retinal detachment and reattachment in primates. *Invest Ophthalmol Vis Sci*. 1990; 31(8):1474-1482.

Gupta P, Yee KM, Garcia P, et al. Vitreoschisis in macular diseases. *Br J Ophthalmol*. 2011; 95(3):376-380.

Hannover A. Entdeckung des Baues des Glaskörpers. *Müller Arch*. 1845; 467-477.

Haritoglou C, Kreutzer T, Tadayoni R, et al. Staining and peeling of the internal limiting membrane using a fluorescent dye (Rhodamine 6 G). *Br J Ophthalmol.* 2008; 92(9):1265-1268.

Haritoglou C, Schumann RG, Kampik A, Gandorfer A. Heavy brilliant blue G for internal limiting membrane staining. *Retina*. 2011; 31(2):405-407.

Harris DE, Warshaw DM, Periasamy M. Nucleotide sequences of the rabbit alpha-smooth-muscle and beta-non-muscle actin mRNAs. *Gene.* 1992; 112(2):265–266.

Heegaard S. Morphology of the vitreoretinal border region. *Acta Ophthalmol Scand Suppl*. 1997; (222):1-31.

Heidenkummer HP, Kampik A. Proliferative activity and immunohistochemical cell differentiation in human epiretinal membranes. *Ger J Ophthalmol*. 1992; 1(3-4):170-175.

Heidenkummer HP, Kampik A. Morphologic analysis of epiretinal membranes in surgically treated idiopathic macular foramina. Results of light and electron microscopy. *Ophthalmologe*. 1996; 93(6):675-679.

Higashimori H, Sontheimer H. Role of Kir4.1 channels in growth control of glia. *Glia*. 2007; 55(16):1668-1679.

Hirayama K, Hata Y, Noda Y, et al. The involvement of the rho-kinase pathway and its regulation in cytokine-induced collagen gel contraction by hyalocytes. *Invest Ophthalmol Vis Sci*. 2004; 45(11):3896-3903.

Hisatomi T, Enaida H, Sakamoto T, et al. A new method for comprehensive bird's-eye analysis of the surgically excised internal limiting membrane. *Am J Ophthalmol*. 2005; 139(6):1121-1122.

Hisatomi T, Enaida H, Sakamoto T, et al. Cellular migration associated with macular hole: a new method for comprehensive bird's-eye analysis of the internal limiting membrane. *Arch Ophthalmol*. 2006; 124(7):1005-1011.

Hiscott PS, Grierson I, Hitchins CA, et al. Epiretinal membranes in vitro. *Trans Ophthalmol Soc U K*. 1983; 103(Pt1):89-102.

Hiscott PS, Grierson I, Trombetta CJ, et al. Retinal and epiretinal glia--an immunohistochemical study. *Br J Ophthalmol*. 1984; 68(10):698-707.

Hiscott P, Waller HA, Grierson I, et al. Local production of fibronectin by ectopic human retinal cells. *Cell Tissue Res*. 1992; 267(1):185-192.

Holness CL, Simmons DL. Molecular cloning of CD68, a human macrophage marker related to lysosomal glycoproteins. *Blood*. 1993; 81(6):1607-1613.

Hönig A, Remy M, Dirisamer M, et al. An in-vivo evaluation of brilliant blue G in macular surgery. *Klin Monbl Augenheilkd*. 2011; 228(8):724-728.

Hu H, Candiello J, Zhang P, et al. Retinal ectopias and mechanically weakened basement membrane in a mouse model of muscle-eye-brain (MEB) disease congenital muscular dystrophy. *Mol Vis*. 2010; 16:1415-1428.

Huang W, Chamberlain CG, Sarafian RY, Chan-Ling T. MHC class II expression by beta2 integrin (CD18)- positive microglia, macrophage and macrophage-like cells in rabbit retina. *Neuron Glia Biol*. 2008; 4(4):285-294.

Huang J, Possin DE, Saari JC. Localizations of visual cycle components in retinal pigment epithelium. *Mol Vis*. 2009 ;15:223-234.

Ibrahim AS, EI-Remessy AB, Matragoon S, et al. Retinal microglial activation and inflammation induced by amadori-glycated albumin in a rat model of diabetes. *Diabetes*. 2011; 60(4):1122-1133.

Ina K, Kitamura H, Tatsukawa S, Fujikura Y. Significance of α-SMA in myofibroblasts emerging in renal tubulointerstitial fibrosis. *Histol Histopathol*. 2011; 26(7):855-866.

Ivanov D, Dvoriantchikova G, Nathanson L, et al. Microarray analysis of gene expression in adult retinal ganglion cells. *FEBS Lett*. 2006; 580(1):331-335.

Jacobsen CH. Epiretinal membranes. *Optom Clin*. 1996 ; 5(1):77-94.

Jahn CE, Minich V, Moldaschel S, Kron M. Perioperative prevalence of epiretinal membranes in eyes with senile cataract. *Klin Monbl Augenheilkd*. 1999 ; 215(4):252-254.

Johnson MW. Posterior vitreous detachment: evolution and complications of its early stages. *Am J Ophthalmol*. 2010; 149(3):371-382.e1.

Kampik A, Green WR, Michels RG, Nase PK. Ultrastructural features of progressive idiopathic epiretinal membrane removed by vitreous surgery. *Am Ophthalmol.* 1980; 90(6):797-809.

Kampik A, Kenyon KR, Michels RG, et al. Epiretinal and vitreous membranes. Comparative study of 56 cases. *Arch Ophthalmol*. 1981; 99(8):1445-1454.

Kaplan R, Morse B, Huebner K, et al. Cloning of three human tyrosine phosphatases reveal a multigene family of receptor-linked protein-tyrosine-phosphatases expressed in brain. *Proc Natl Acad Sci U S A*. 1990; 87(18):7000-7004.

Katira RC, Zamani M, Berinstein DM, Garfinkel RA. Incidence and characteristics of macular pucker formation after primary retinal detachment repair by pars plana vitrectomy alone. *Retina*. 2008; 28(5):744-748.

Kelly NE, Wendel RT. Vitreous surgery for idiopathic macular holes. Results of a pilot study. *Arch Ophthalmol*. 1991; 109(5): 654-659.

Khazen W, M'bika JP, Tomkiewicz C, et al. Expression of macrophage-selective markers in human and rodent adipocytes. *FEBS Lett.* 2005; 579(25):5631–5634.

Khoshnoodi J, Pedchenko V, Hudson BG. Mammalian collagen IV. *Microsc Res Tech.* 2008; 71(5):357–370.

Koerner F, Garweg J. Vitrectomy for macular pucker and vitreomacular traction syndrome. *Doc Ophthalmol*. 1999; 97(3-4):449-458.

Kohno RI, Hata Y, Kawahara S, et al. Possible contribution of hyalocytes to idiopathic epiretinal membrane formation and its contraction. *Br J Ophthalmol.* 2009; 93(8):1020-1026.

Kreutzberg GW. Microglia, the first line of defense in brain pathologies. *Arzneimittelforschung*. 1995; 45(3A):357-360.

Kusik BW, Hammond DR, Udvadia AJ. Transcriptional regulatory regions of gap43 needed in developing and regenerating retinal ganglion cells. *Dev Dyn*. 2010; 239(2):482-495.

Kwok AK, Lai TY, Li WW, et al. Indocyanine green-assisted internal limiting membrane removal in epiretinal membrane surgery: a clinical and histologic study. *Am J Ophthalmol*. 2004; 138(2):194-199.

Kwok AKh, Lai TY, Yuen KS. Epiretinal membrane surgery with or without internal limiting membrane peeling. *Clin Experiment Ophthalmol*. 2005; 33(4):379-385.

Lazarus HS, Hageman GS. In situ characterization of the human hyalocytes. *Arch Ophthalmol*. 1994; 112(10):1356-1362.

Lee EG, Pang TW, Nelson J, et al. Comparison of mounting methods for the evaluation of fibers by phase contrast microscopy. *Ann Occup Hyg*. 2011; 55(6): 644-657.

Lesnik Oberstein SY, Lewis GP,Chapin EA, Fisher SK. Ganglion cell neurites in human idiopathic epiretinal membranes. *Br J Ophthalmol*. 2008; 92(7):981-985.

Lesnik Oberstein SY, Lewis GP, Dutra T, Fisher SK. Evidence that neurites in human epiretinal membranes express melanopsin, calretinin, rod opsin and neurofilament protein. *Br J Ophthalmol*. 2011; 95(2):266-272.

Lewis GP, Fisher SK. Up-regulation of glial fibrillary acidic protein in response to retinal injury: its potential role in glial remodeling and a comparison to vimentin expression. *Int Rev Cytol.* 2003; 230:263-290.

Li R, Maminishkis A, Zahn G, et al. Integrin alpha5beta1 mediates attachment, migration, and proliferation in human retinal pigment epithelium: relevance for proliferative retinal disease. *Invest Ophthalmol Vis Sci*. 2009; 50(12):5988-5996.

Limb GA, Salt TE, Munro PM, et al. In vitro characterization of a spontaneously immortalized human Müller cell line (MIO-M1). *Invest Ophthalmol Vis Sci*. 2002; 43(3):864-869.

Liu H, Kao WW. A novel protocol of whole mount electro-immunofluorescence staining. *Mol Vis*.2009; 15:505-517.

Llombart C, Nacher V, Ramos D, et al. Morphological characterization of pecteneal hyalocytes in the developing quail retina. *J Anat*. 2009; 215(3):280-291.

Luna G, Lewis GP, Banna CD, et al. Expression profiles of nestin and synemin in reactive astrocytes and Müller cells following retinal injury: a comparison with glial fibrillar acidic protein and vimentin. *Mol Vis*. 2010; 16:2511-2523.

Manduch M, Dexter DF, Jalink DW, et al. Undifferentiated pancreatic carcinoma with osteoclast-like giant cells: Report of a case with osteochondroid differentiation. *Pathol Res Pract*. 2009; 205(5):353–359.

Maw MA, Kennedy B, Knight A, et al. Mutation of the gene encoding cellular retinaldehyde-binding protein in autosomal recessive retinitis pigmentosa. *Nat Genet*. 1997; 17(2):198–200.

McDonald HR, Johnson RN, Schatz H. Surgical results in the vitreomacular traction syndrome. *Ophthalmology*. 1994; 101(8):1397-1402; discussion 1403..

Meth RD, Thompson EB. Hormonal regulation of physiological cell turnover and apoptosis. *Cell Tissue Res*. 2000; 301(1):101-124.

Middeldorp J, Hol EM. GFAP in heath and disease. *Prog Neurobiol*. 2011; 93(3):421-423.

Morales MC, Freire V, Asumendi A, et al. Comparative effects of six intraocular vital dyes on retinal pigment epithelial cells. *Invest Ophthalmol Vis Sci*. 2010; 51(11):6018-6029.

Morris R, Witherspoon CD. In: Kriegelstein G, ed. Retinology Today. Munich, Germany: Verlag fuer Medizin und Naturwissenschaftler. 2000; 83-88.

Nakazawa T, Takeda M, Lewis GP, et al. Attenuated glial reactions and photoreceptor degeneration after retinal detachment in mice deficient in glial fibrillary acidic protein and vimentin. *Invest Ophthalmol Vis Sci*. 2007; 48(6):2760-2768.

Nishitsuka K, Kashiwagi Y, Toji N, et al. Hyaluronan production regulation from porcine hyalocyte cell line by cytokines. *Exp Eye Res*. 2007; 85(4):539-545.

Ng TF, Turpie B, Masli S. Thrombospondin-1-mediated regulation of microglia activation after retinal injury. *Invest Ophthalmol Vis Sci*. 2009; 50(11):5472-5478.

Nishitsuka K, Kashiwagi Y, Tojo N, et al. Hyaluronan production regulation from porcine hyalocyte cell line by cytokines. *Exp Eye Res*. 2007; 85(4):539-545.

Pankov R, Yamada KM. Fibronectin at a glance. *J Cell Sci*. 2002; 115(Pt 20):3861–3863.

Park DW, Dugel DU, Garda J, et al. Macular pucker removal with and without internal limiting membrane peeling: pilot study. *Ophthalmology*. 2003; 110(1):62-64.

Ponsioen TL, van Luyn MJ, van der Worp RJ, et al. Collagen distribution in the human vitreoretinal interface. *Invest Ophthalmol Vis Sci.* 2008; 49(9):4089-4095.

Ramesh S, Bonshek RE, Bishop PN. Immunolocalisation of opticin in the human eye. *Br J Ophthalmol*. 2004; 88(5):697-702.

Ramírez JM, Triviño A, Ramírez AI, et al. Structural specializations of human retinal glial cells. *Vision Res*. 1996; 36(14):2029-2036.

Qiao H, Hisatomi T, Sonoda KH, et al. The characterisation of hyalocytes: the origin, phenotype, and turnover. *Br J Ophthalmol*. 2005 ; 89(4):513-517.

Rodrigues EB, Meyer CH, Kroll P. Chromovitrectomy: a new filed in vitreoretinal surgery. *Graefes Arch Clin Exp Ophthalmol.* 2005; 243(4):291-293.

Roy S, Cagliero E, Lorenzi M. Fibronectin overexpression in retinal microvessels of patients with diabetes. *Invest Ophthalmol Vis Sci*. 1996; 37(2):258-266.

Ruiz-Ederra J, Zhang H, Verkman AS. Evidence against functional interaction between aquaporin-4 water channels and Kir4.1 potassium channels in retinal Müller cells. *J Biol Chem*. 2007; 282(30): 21866-21872.

Sakamoto T. Cell biology of hyalocytes. *Nihon Ganka Gakkai Zasshi.* 2003; 107(12):866-882; discussion 883.

Sakamoto T, Ishibashi T. Hyalocytes: essential cells of the vitreous cavity in vitreoretinal pathophysiology? *Retina*. 2011; 31(2):222-228.

Sandercoe TM, Madigan MC, Billson FA, et al. Astrocyte proliferation during development of the human retinal vasculature. *Exp Eye Res*. 1999; 69(5):511-523.

Satterthwaite AB, Burn TC, Le Beau MM, Tenen DG. Structure of the gene encoding CD34, a human hematopoietic stem cell antigen. *Genomics.* 1992; 12(4):788–794.

Schmitt S, Aftab U, Jiang C, et al. Molecular characterization of human retinal progenitor cells. *Invest Ophthalmol Vis Sci*. 2009; 50(12):5901-5908.

Schonk DM, Kuijpers HJ, van Drunen E, et al. Assignment of the gene(s) involved in the expression of the proliferation-related Ki-67 antigen to human chromosome 10. *Hum Genet*. 1989; 83(3):297–299.

Schumann RG, Schaumberger MM, Rohleder M, et al. Ultrastructure of the vitreomacular interface in full-thickness idiopathic macular holes: a consecutive analysis of 100 cases. *Am J Ophthalmol*. 2006; 141(6):1112-1119.

Schumann RG, Schaumberger MM, Rohleder M, et al. The primary objective in macular hole surgery. Ultrastructural features of the vitreomacular interface. *Ophthalmologe*. 2007; 104(9):783-789.

Schumann RG, Rohleder M, Schaumberger MM, et al. Idiopathic macular holes: ultrastructural aspects of surgical failure. *Retina*. 2008; 28(2):340-349.

Schumann RG, Gandorfer A, Priglinger SG, et al. Vital dyes for macular surgery: a comparative electron microscopy study of the internal limiting membrane. *Retina*. 2009; 29(5):669-676.

Schumann RG, Gandorfer A, Eibl KH, et al. Sequential epiretinal membrane removal with internal limiting membrane peeling in brilliant blue G-assisted macular surgery. *Br J Ophthalmol*. 2010; 94(10):1369-1372.

Schumann RG, Eibl KH, Zhao F, et al. Immunocytochemical and ultrastructural evidence of glial cells and hyalocytes in internal limiting membrane specimens of idiopathic macular holes. *Invest Ophthalmol Vis Sci*. 2011; 52(11):7822-7834.

Scott JE. The chemical morphology of the vitreous. *Eye (Lond).* 1992; 6(Pt 6):553-555.

Sebag J, Balazs EA. Morphology and ultrastructure of human vitreous fibers. *Invest Ophthalmol Vis Sci*. 1989; 30(8):1867-1871.

Sebag J. Age-related differences in the human vitreoretinal interface. *Arch Ophthalmol*. 1991; 109(7):966-971.

Sebag J. The vitreous. In: Hart W, ed. *Adlers Physiology of the Eye*, 9th edn. 1992. St. Louis: Mosby Year Book.

Sebag J. Anomalous posterior vitreous detachment: a unifying concept in vitreo-retinal disease. *Graefes Arch Clin Exp Ophthalmol*. 2004; 242(8):690-698.

Sebag J, Gupta P, Rosen RR, et al. Macular holes and macular pucker: the role of vitreoschisis as imaged by optical coherence tomography/scanning laser ophthalmoscopy. *Trans Am Ophthalmol Soc*. 2007; 105:121-129.

Sebag J. Vitreochisis. *Graefes Arch Clin Exp Ophthalmol*. 2008; 246(3):329–332.

Semple-Rowland SL, Coggin WE, Geesey M, et al. Expression characteristics of dual-promoter lentiviral vectors targeting retinal photoreceptors and Müller cells. *Mol Vis.* 2010; 16:916-934.

Sethi CS, Lewis GP, Fisher SK, et al. Glial remodeling and neural plasticity in human retinal detachment with proliferative vitreoretinopathy. *Invest Ophthalmol Vis Sci*. 2005; 46(1):329-342.

Shechtman DL, Dunbar MT. The expanding spectrum of vitreomacular traction. *Optometry*. 2009; 80(12):681-687.

Shinoda K, Hirakata A, Hida T, et al. Ultrastructural and immunohistochemical findings in five patients with vitreomacular traction syndrome. *Retina*. 2000; 20(3):289-293.

Simmons DL, Satterthwaite AB, Tenen DG, Seed B. Molecular cloning of a cDNA encoding CD34, a sialomucin of human hematopoietic stem cells. *J Immunol*. 1992; 148(1):267–271.

Smiddy WE, Maguire AM, Green WR, et al. Idiopathic epiretinal membranes. Ultrastructural characteristics and clinicopathologic correlation. *Ophthalmology*. 1989; 96(6):811-820; discussion 821.

Smiddy WE, Michels RG, Gilbert HD, Green WR. Clinicopathologic study of idiopathic macular pucker in children and young adults. *Retina*. 1992; 12(3):232-236.

Snead DR, Cullen N, James S, et al. Hyperconvolution of the inner limiting membrane in vitreomaculopathies. *Graefes Arch Clin Exp Ophthalmol*. 2004; 242(10):853-862.

Strauss O. The role of retinal pigment epithelium in visual functions. *Ophthalmologe*. 2009; 106(4):299-304.

Streit WJ. Microglia and macrophages in the developing CNS. *Neurotoxicology*. 2001; 22(5): 619-624.

Sugita S. Role of ocular pigment epithelial cells in immune privilege. *Arch Immunol Ther Exp (Warsz)*. 2009; 57(4):263-268.

Sugita S, Horie S, Yamada Y, Mochizuki M. Inhibition of B-cell activation by retinal pigment epithelium. *Invest Ophthalmol Vis Sci*. 2010; 51(11):5783-5788.

Tari SR, Vidne-Hay O, Greenstein VC, et al. Functional and structural measurements for the assessment of internal limiting membrane peeling in idiopathic macular pucker. *Retina*. 2007; 27(5):567-572.

Timpl R, Rohde H, Robey PG, et al. Laminin--a glycoprotein from basement membranes. *J Biol Chem*. 1979; 254(19):9933-9937.

Trese M, Chandler DB, Machemer R. Macular pucker II. Ultrastructure. *Graefes Arch Clin Ophthalmol*. 1983; 221(1):16-26.

Uchida H, Hayashi H, Kuroki M, et al. Vitamin A up-regulates the expression of thrombospondin-1 and pigment epithelium-derived factor in retinal pigment epithelial cells. *Exp Eye Res*. 2005; 80(1):23-30.

Uhlmann S, Bringmann A, Uckermann O, et al. Early glial cell reactivity in experimental retinal detachment : effect of suramin. *Invest Ophthalmol Vis Sci*. 2003; 44(9):4114-4122.

Vinores SA, Campochiaro PA, Conway BP. Ultrastructural and electron-immunocytochemical characterization of cells in epiretinal membranes. *Invest Ophthalmol Vis Sci*. 1990 ; 31(1):14-28.

Walcott JC, Provis JM. Müller cells express the neuronal progenitor cell marker nestin in both differentiated and undifferentiated human foetal retina. *Clin Experiment Ophthalmol*. 2003; 31(3):246-249.

Wang D, Hazell AS. Microglial activation is a major contribution to neurologic dysfunction in thiamine deficiency. *Biochem Biophys Res Commun*. 2010; 402(1):123-128.

Watanabe T, Raff MC. Retinal astrocytes are immigrants from the optic nerve. *Nature*. 1988; 332(6167):834-837.

Wylegala E, Woyna-Orlewicz A, Pilat J, et al. Traction maculopathies—pathogenesis and diagnostics. *Klin Oczna*. 2006; 108(10-12):457-463.

Yang P, Das PK, Kijldtra A. Localization and characterization of immunocompetent cells in the human retina. *Ocul Immunol Inflamm*. 2000; 8(3):149-157.

Yang P, Chen L, Zwart R, Kijlstra A. Immune cells in the porcine retina: distribution, characterization and morphological features. *Invest Ophthalmol Vis Sci*. 2002; 43(5):1488-1492.

Zarbin MA, Michels RG, Green WR. Epiretinal membrane contracture associated with macular prolapse. *Am J Ophthalmol*. 1990; 110(6):610-618.

Zeng HY, Green WR, Tso Mo. Microglial activation in human diabetic retinopathy. *Arch Ophthalmol*. 2008; 126(2):227-232.

Zhang J, Shan Q, Ma P, et al. Differentiation potential of bone marrow mesenchymal stem cells into retina in normal and laser-injured rat eye. *Sci China C Life Sci*. 2004; 47(3):241-250.

Zhu M, Provis JM, Penfold PL. The human hyaloid system: cellular phenotypes and inter-relationships. *Exp Eye Res*. 1999; 68(5):553-563.

C. Appendix

C.1 Acknowledgement

When I left China for Germany at the end of October 2009, my parents probably were the happier parents on the earth, even with the chinese tradition that a grown-up daughter is better to stay by aging parents as a walking stick. I left them, and they gave me the biggest support instead of complaints. My dearest mother and father, I am so proud to have you as my parents. My lovely husband, thank you so much for being there supporting and encouraging me, I really miss you. And my dearest parents-in-law, thank you for giving me selfless love. How I am lucky to have you as family, I really appreciate and I love you.

Before I came to Germany, I would have been lost without instructions that Dr. Matthias Hadesbeck from foreign affair office in Ludwig-Maximilians-University provided me with. I sincerely thank you so much.

Prof. Dr. med. Anselm Kampik, I would like to take the opportunity to thank you for the friendly scientific environment in the Eye Hospital of the Ludwig-Maximilians-University Munich. I am also grateful for your erudition and preciseness. I truly appreciate the opportunity to finish my doctoral study under your supervision and guidance.

Prof. Dr. med. Arnd Gandorfer, I want to thank you sincerely for your constant support and the motivations that you have been providing me with, and for your inspiration to encourage me to be with an open and positive mind. I appreciate all your hard work, it’s meant so much to me, and if I may, a great and lifelong mentor in matters of life.

Dr. med. Ricarda G. Schumann, with your great help I could learn more skills and involve with more interesting studies. And of course, thank you so much for your massive and selfless contributions in making this dissertation and the paper appear the way they are. I am so lucky to have you as a wonderful mate and a great friend in my life. Sincerely wish you all the best!

Studying medicine in China is probably not the best of backgrounds to start laboratory research in Germany. Mrs. Renate Scheler, you taught me almost everything what I know of laboratory work. Thank you for being a great friend in my life.

Dr. med. Yang Yang, you have been an warm-hearted companion, helping me to rent the apartment when I came here at the beginning, providing me with tips and tricks that you have helped me out with, from troubles with things including computers. Thank you so much!

Lovely Mrs. Serbin and Mrs. Pressler, thank you for your kindly help in the lab. Wish you enjoy the pasta with chopsticks ^_^

Special thanks to Prof. Dr. med. Christos Haritoglou and Dr. med. M. Grüterich who provide the specimens and to Dr. rer. biol. hum. Dipl.-Phys. Markus M. Schaumberger who helped me get through with computer.

Many thanks also to all of you, in the lab and outside who have made life, at different periods in time, a joy to live.

Fei 赵菲

C.2 Curriculum Vitae

Name
Zhao, Fei

Citizenship
Chinese

Date of Birth
17th of March, 1982

Place of Birth
Tianjin, China

Marital Status
Married

Home Address
No.301, Yanchang Rd., Shanghai 200072, China

Present Address
W15, Connollystr.3, Munich 80809, Germany

Education
Primary School (Sep.1988- Jun.1994)
Weididao Primary School, Tianjin, China

Middle School (Sep.1994- Jun.1997)
Tongren Girls Middle School, Tianjin, China

High school (Sep.1997- Jun.2000)
Yaohua High School, Tianjin, China

Bachelor of Medicine and Master of Medicine (Ophthalmic Specialty) (Sep.2000- Jun.2008)
Tongji University, Shanghai, China

Conferral of the Doctor of Medicine Degree (Promotion (Medizin)) (since Oct.2009)
Eye Hospital of the Ludwig-Maximilians-University Munich, Germany

Professional Experience
Ophthalmology residency (Jul. 2008- Sep. 2009)
Department of Ophthalmology, Shanghai Tenth People's Hospital of Tongji University, China

Certificate of Licensed Practicing Physician (China) (Sep.2008)